



**HAL**  
open science

## Reaffirmation of Mechanistic Proteomic Signatures Accompanying SGLT2 Inhibition in Patients With Heart Failure

Milton Packer, João Pedro Ferreira, Javed Butler, Gerasimos Filippatos,  
James L Januzzi, Sandra González Maldonado, Marina Panova-Noeva, Stuart  
J Pocock, Jürgen H Prochaska, Maral Saadati, et al.

► **To cite this version:**

Milton Packer, João Pedro Ferreira, Javed Butler, Gerasimos Filippatos, James L Januzzi, et al..  
Reaffirmation of Mechanistic Proteomic Signatures Accompanying SGLT2 Inhibition in Patients  
With Heart Failure. *Journal of the American College of Cardiology*, 2024, Online ahead of print.  
10.1016/j.jacc.2024.07.013 . hal-04694584

**HAL Id: hal-04694584**

**<https://hal.univ-lorraine.fr/hal-04694584v1>**

Submitted on 11 Sep 2024

**HAL** is a multi-disciplinary open access archive for the deposit and dissemination of scientific research documents, whether they are published or not. The documents may come from teaching and research institutions in France or abroad, or from public or private research centers.

L'archive ouverte pluridisciplinaire **HAL**, est destinée au dépôt et à la diffusion de documents scientifiques de niveau recherche, publiés ou non, émanant des établissements d'enseignement et de recherche français ou étrangers, des laboratoires publics ou privés.

# Reaffirmation of Mechanistic Proteomic Signatures Accompanying SGLT2 Inhibition in Patients With Heart Failure

## A Validation Cohort of the EMPEROR Program

Milton Packer, MD,<sup>a,b</sup> João Pedro Ferreira, MD, PhD,<sup>c,d</sup> Javed Butler, MD, MPH,<sup>d,e</sup> Gerasimos Filippatos, MD, PhD,<sup>f</sup> James L. Januzzi, Jr, MD,<sup>f,g</sup> Sandra González Maldonado, PhD,<sup>h</sup> Marina Panova-Noeva, MD, PhD,<sup>i,j</sup> Stuart J. Pocock, PhD,<sup>k</sup> Jürgen H. Prochaska, MD,<sup>l,m</sup> Maral Saadati, PhD,<sup>n</sup> Naveed Sattar, MD, PhD,<sup>o</sup> Mikhail Sumin, MD, PhD,<sup>l</sup> Stefan D. Anker, MD,<sup>p</sup> Faiez Zannad, MD, PhD<sup>q,r</sup>

### ABSTRACT

**BACKGROUND** Sodium-glucose cotransporter 2 (SGLT2) inhibitors exert a distinctive pattern of direct biological effects on the heart and kidney under experimental conditions, but the meaningfulness of these signatures for patients with heart failure has not been fully defined.

**OBJECTIVES** We performed the first mechanistic validation study of large-scale proteomics in a double-blind randomized trial of any treatment in patients with heart failure.

**METHODS** In a discovery cohort from the EMPEROR (Empagliflozin Outcome Trial in Patients With Chronic Heart Failure and Reduced Ejection Fraction) program, we studied the effect of randomized treatment with placebo or empagliflozin on 1,283 circulating proteins in 1,134 patients with heart failure with a reduced or preserved ejection fraction. In a validation cohort, we expanded the number to 2,155 assessed proteins, which were measured in 1,120 EMPEROR participants who had not been studied previously.

**RESULTS** In the validation cohort, 25 proteins were the most differentially enriched by empagliflozin (ie,  $\geq 15\%$  between-group difference and false discovery rate  $< 1\%$  at 12 weeks with known effects on the heart or kidney): 1) 13 proteins promote autophagy and other cellular quality-control functions (IGFBP1, OTUB1, DNAJB1, DNAJC9, RBP2, IST1, HSPA8, H-FABP, FABP6, ATP1F1, TfR1, EPO, IGBP1); 2) 12 proteins enhance mitochondrial health and ATP production (UMtCK, TBCA, L-FABP, H-FABP, FABP5, FABP6, RBP2, IST1, HSPA8, ATP1F1, TfR1, EPO); 3) 7 proteins augment cellular iron mobilization or erythropoiesis (TfR1, EPO, IGBP1, ERMAP, UROD, ATP1F1, SNCA); 4) 3 proteins influence renal tubular sodium handling; and 5) 9 proteins have restorative effects in the heart or kidneys, with many proteins exerting effects in  $> 1$  domain. These biological signatures replicated those observed in our discovery cohort. When the threshold for a meaningful between-group difference was lowered to  $\geq 10\%$ , there were 58 additional differentially enriched proteins with actions on the heart and kidney, but the biological signatures remained the same.

**CONCLUSIONS** The replication of mechanistic signatures across discovery and validation cohorts closely aligns with the experimental effects of SGLT2 inhibitors. Thus, the actions of SGLT2 inhibitors—to promote autophagy, restore mitochondrial health and production of ATP, promote iron mobilization and erythropoiesis, influence renal tubular ion reabsorption, and normalize cardiac and renal structure and function—are likely to be relevant to patients with heart failure. (EMPagliflozin outcomE tRial in Patients With chrOnic heaRt Failure With Preserved Ejection Fraction [EMPEROR-Preserved], [NCT03057951](https://doi.org/10.1016/j.jacc.2024.07.013); EMPagliflozin outcomE tRial in Patients With chrOnic heaRt Failure With Reduced Ejection Fraction [EMPEROR-Reduced], [NCT03057977](https://doi.org/10.1016/j.jacc.2024.07.013)) (JACC. 2024; ■:■-■) © 2024 The Authors. Published by Elsevier on behalf of the American College of Cardiology Foundation. This is an open access article under the CC BY-NC-ND license (<http://creativecommons.org/licenses/by-nc-nd/4.0/>).

**ABBREVIATIONS  
AND ACRONYMS****eGFR** = estimated glomerular filtration rate**FDR<sub>q</sub>** = false discovery rate adjusted *P* value**MMRM** = mixed models for repeated measurements**NHE3** = sodium-hydrogen exchanger 3**SGLT2** = sodium-glucose cotransporter 2

Sodium-glucose cotransporter 2 (SGLT2) inhibitors reduce the risk of cardiovascular death and hospitalization for heart failure in patients with heart failure, both with reduced and preserved ejection fraction.<sup>1</sup> Potential mechanisms of action have been elucidated in both experimental models and in the clinical setting. Experimentally, SGLT2 inhibitors have been shown to reduce oxidative and other cellular stresses, mute inflammation, and fibrosis and enhance the cellular housekeeping process known as autophagy.<sup>2,3</sup> SGLT2 inhibitors also restore mitochondrial health and biogenesis while enhancing fatty acid oxidation: actions that augment the production of adenosine triphosphate (ATP).<sup>4</sup> Clinically, the administration of SGLT2 inhibitors is accompanied by a transient natriuresis, augmented erythrocytosis and iron mobilization, and restoration of cardiac structure and function.<sup>5-7</sup>

In a discovery analysis of the EMPEROR (Empagliflozin Outcome Trial in Patients With Chronic Heart Failure With Reduced or Preserved Ejection Fraction) program,<sup>8</sup> we studied the effect of empagliflozin on 1,283 circulating proteins in 1,134 patients with heart failure with reduced or preserved ejection fraction. The most common biological actions of differentially enriched proteins in the heart were to promote autophagic flux; to reduce oxidative stress, inhibit inflammation and fibrosis, and enhance mitochondrial health; and to promote repair and regenerative capacity. The actions of differentially enriched proteins in the kidney involved enhanced autophagy; suppression of renal inflammation and

fibrosis; and modulation of renal tubular sodium reabsorption.

In the current validation analysis, we expanded the number of assessed proteins to 2,155; furthermore, we performed the measurements in 1,120 patients from the EMPEROR program who had not been included in our discovery cohort. These extended assessments provided an opportunity not only to confirm or refute our previous findings but also to identify additional differentially enriched proteins that might support previously identified mechanistic proteomic signatures or would reflect effects of SGLT2 inhibitors that have demonstrated either in the experimental or clinical setting. To our knowledge, the current analyses represent the first study to reaffirm the mechanistic proteomics signature in response to any treatment for heart failure in a validation cohort studied under the same conditions as the discovery cohort.

**METHODS****STUDY POPULATION AND BIOSAMPLING PROCEDURES.**

A total of 9,718 patients were enrolled in the EMPEROR-Reduced (n = 3,730) and EMPEROR-Preserved (n = 5,988) trials. Participation in the sampling for biobanking of plasma, serum, DNA, and urine was voluntary. Biosamples were collected only after a separate informed consent had been signed, in accordance with local ethical and regulatory requirements and approval of Institutional Review Boards. The principles and methodology for biobanking in EMPEROR trials are described in the [Supplemental Methods 1](#). In the EMPEROR-Reduced

From the <sup>a</sup>Baylor Heart and Vascular Institute, Baylor University Medical Center, Dallas, Texas, USA; <sup>b</sup>Imperial College London, London, United Kingdom; <sup>c</sup>UnIC@RISE, Cardiovascular Research and Development Center, Department of Surgery and Physiology, Faculty of Medicine of the University of Porto, Porto, Portugal; <sup>d</sup>Baylor Scott and White Research Institute, Dallas, Texas, USA; <sup>e</sup>University of Mississippi Medical Center, Jackson, Mississippi, USA; <sup>f</sup>National and Kapodistrian University of Athens School of Medicine, Athens University Hospital Attikon, Athens, Greece; <sup>g</sup>Massachusetts General Hospital and Bain Institute for Clinical Research, Boston, Massachusetts, USA; <sup>h</sup>Boehringer Ingelheim Pharma GmbH & Co KG, Biberach, Germany; <sup>i</sup>Boehringer Ingelheim Pharma GmbH & Co KG, Ingelheim, Germany; <sup>j</sup>Center for Thrombosis and Haemostasis, University Medical Center, Johannes Gutenberg University Mainz, Mainz, Germany; <sup>k</sup>London School of Hygiene and Tropical Medicine, London, United Kingdom; <sup>l</sup>Boehringer Ingelheim International GmbH, Ingelheim, Germany; <sup>m</sup>Preventive Cardiology and Preventive Medicine, Department of Cardiology, University Medical Center of the Johannes Gutenberg University Mainz, Mainz, Germany; <sup>n</sup>Elderbrook Solutions GmbH, on behalf of Boehringer Ingelheim Pharma GmbH & Co KG, Biberach an der Riss, Germany; <sup>o</sup>Institute of Cardiovascular and Medical Sciences, University of Glasgow, Glasgow, United Kingdom; <sup>p</sup>Department of Cardiology (CVK) of German Heart Center Charité, Institute of Health Center for Regenerative Therapies (BCRT), German Centre for Cardiovascular Research (DZHK) partner site Berlin, Charité Universitätsmedizin, Berlin, Germany; <sup>q</sup>Centre d'Investigations Cliniques Plurithématique 1433, INSERM, Université de Lorraine, Nancy, France; and the <sup>r</sup>F-CRIN INI-CRCT (Cardiovascular and Renal Clinical Trialists), INSERM U1116, Centre Hospitalier Régional Universitaire de Nancy, Nancy, France.

The authors attest they are in compliance with human studies committees and animal welfare regulations of the authors' institutions and Food and Drug Administration guidelines, including patient consent where appropriate. For more information, visit the [Author Center](#).

trial, 1,963 patients consented to provide biosamples, of which 1,463 had samples available at baseline and at least at 1 on-treatment follow-up visit (after 12 weeks or 52 weeks). In the EMPEROR-Preserved trial, of the 3,831 patients who consented for biosampling, 3,067 had samples available at baseline and at 1 or more additional follow-up visits.

In our previous discovery cohort, we analyzed the proteomic signatures in 1,134 patients (Cohort 1) using the Olink Explore 1536 platform (Thermo Fisher Scientific), and in the current validation study, we analyzed blood samples using the Olink Explore 3072 platform in 1,120 patients not included in our previous report (validation Cohort 2). Plasma samples of 582 patients (of 863) in the EMPEROR-Reduced trial and of 538 (of 2,528) in the EMPEROR-Preserved trial who were not included in our previous report were randomly selected for analysis, stratifying for treatment assignment and data availability. In both cohorts, measurements of circulating proteins were performed using proximity extension assay technology with a dual-recognition DNA-coupled readout, in which oligonucleotide-labeled antibody probe pairs are allowed to bind to their respective targets.<sup>9</sup> Overlapping assays (eg, interleukins and tumor necrosis factor family proteins) were included as a quality control. The platform provides log<sub>2</sub> normalized protein enrichment values with relative quantification. Bridging samples (that are common to the 2 cohorts) are assayed to harmonize normalized units across the 2 sets of data.

The assays were performed blinded to the treatment allocation. All proteins measured in the Olink Explore 1536 platform were also assayed in the Olink Explore 3072 platform. Missing values were observed when samples failed quality control (as specified by the manufacturer) and were not imputed. Proteins with >33% of baseline samples below the reliable limit of detection were excluded from the analysis, and thus a total of 2,155 proteins (of 2,945 evaluated) proteins were assessed in validation Cohort 2.

**STATISTICAL ANALYSES.** Changes from baseline at 12 and 52 weeks were measured in both the placebo and empagliflozin groups, and between-group differences were calculated at both time points. Because of the multiplicity of analyses, we did not rely on conventional *P* values but instead estimated a false discovery rate adjusted *P* value (FDRq) <1% (adjusted *P* < 0.01), using a Benjamini-Hochberg correction.<sup>10</sup> In addition, we determined that a between-group difference was of interest if it was ≥10% (equivalent to a |log<sub>2</sub> fold change| > 0.1375) or ≥15% (equivalent to a |log<sub>2</sub> fold change| > 0.2016), both with a FDRq <1%

(FDR-adjusted *P* < 0.01). These thresholds are the same as those used in our previous report.<sup>8</sup> These criteria were used to define the identification of a differentially enriched protein as a result of treatment with empagliflozin.

Changes in proteins over time were assessed using mixed models for repeated measurements (MMRM), which compared the change in plasma concentrations for each protein from baseline to 12 and to 52 weeks between treatment groups (empagliflozin vs placebo), while adjusting for the protocol-prespecified baseline covariates (ie, age, sex, geographic region, diabetes, left ventricular ejection fraction, estimated glomerular filtration rate [eGFR]), and the baseline protein level. Analysis of pooled EMPEROR data included the study indicator as an additional covariate. Furthermore, unless otherwise specified, all changes were adjusted for changes in eGFR at 12 weeks,<sup>8</sup> as SGLT2 inhibitors may reduce glomerular filtration early in treatment, and this reduction may influence the renal clearance of circulating proteins. In the MMRM models, differences between effects at weeks 12 and 52 were investigated by a treatment-by-visit interaction term, and differences in patients in the EMPEROR-Reduced and EMPEROR-Preserved trials were assessed by a treatment-by-study interaction term, both with a FDRq <1%.

## RESULTS

**PATIENT CHARACTERISTICS.** The demographic and clinical features of the 1,134 patients in discovery Cohort 1 were similar to the 1,120 patients in the validation Cohort 2 (Supplemental Table 1).

**FINDINGS OF DIFFERENTIALLY ENRICHED PROTEINS. Proteins showing between-group difference ≥10% with FDRq <1% at 12 weeks.** After 12 weeks of randomized treatment in our validation Cohort 2, 117 proteins were increased by ≥10% in the empagliflozin group (compared with the placebo group) after adjustment for change in eGFR (|log<sub>2</sub> fold change| > 0.1375) and with a FDRq <1% (FDR adjusted *P* < 0.01) (Supplemental Table 2). The effects in patients with a reduced and a preserved ejection fraction were not significantly different from each other, all FDRq >1%.

By contrast, based on a more limited number of proteins analyzed in our discovery Cohort 1, we had identified only 32 proteins that showed a ≥10% treatment difference with a FDRq <1% (FDR adjusted *P* < 0.01) at 12 weeks, and only 16 proteins that showed a ≥10% treatment effect with a FDRq <1% at 12 weeks, after adjustment for the change in eGFR.<sup>8</sup>

**TABLE 1** Reproducibility of the Magnitude of Between-Group Protein Enrichment Among 72 Proteins That Were Deemed to Be Differentially Enriched in Either in the Discovery Cohort 1 or in the Validation Cohort 2 and Were Measured in Both Cohorts

	UniProt ID	Log <sub>2</sub> Fold Change  (95% CI)	
		Discovery Cohort 1 (Olink 1536 Platform)	Validation Cohort 2 (Olink 3072 Platform)
Mitochondrial ATPase inhibitor	Q9UII2	0.16 (-0.02 to 0.34)	0.31 (0.13-0.49)
Retinol-binding protein 2	P50120	0.15 (0.05-0.24)*	0.30 (0.21-0.39)
DnaJ homolog subfamily B member 1	P25685	0.20 (0.02-0.38)	0.26 (0.10-0.42)
Fatty acid-binding protein, liver	P01748	0.13 (0.01-0.26)	0.25 (0.14-0.36)
Creatine kinase U-type, mitochondrial	P12532	0.22 (0.11-0.33)*†	0.25 (0.12-0.37)
C-C motif chemokine 5	P13501	0.24 (0.08-0.41)	0.25 (0.10-0.41)
C-C motif chemokine 28	Q9NRJ3	0.07 (-0.01 to 0.15)	0.23 (0.14-0.33)
Fatty acid-binding protein 5	Q01469	0.16 (0.05-0.27)	0.23 (0.12-0.33)
Transferrin receptor protein 1	P02786	0.25 (0.18-0.32)*†	0.22 (0.16-0.28)
Carbonic anhydrase 2	P00918	0.26 (0.12-0.40)*	0.22 (0.09-0.35)
Insulin-like growth factor binding protein 1	P08833	0.25 (0.13-0.38)*†	0.22 (0.09-0.36)
Gastrotropin	P51161	0.11 (0.02-0.20)	0.21 (0.12-0.29)
Erythropoietin	P01588	0.24 (0.10-0.37)*	0.21 (0.09-0.33)
Protein-glutamine g-glutamyltransferase 2	P21980	0.25 (0.12-0.38)*	0.21 (0.06-0.35)
Serine protease inhibitor Kazal-type 4	O60575	0.11 (0.04-0.18)	0.20 (0.13-0.26)
Ghrelin	Q9UBU3	0.09 (0.00-0.18)	0.20 (0.11-0.29)
Oncostatin-M	P13725	0.15 (0.04-0.26)	0.20 (0.08-0.32)
Thymosin beta-10	P63313	0.19 (0.08-0.31)*	0.20 (0.08-0.31)
Uromodulin	P07911	0.18 (0.12-0.23)*†	0.19 (0.14-0.24)
CEA-related cell adhesion molecule 8	P31997	0.06 (-0.02 to 0.15)	0.19 (0.10-0.29)
C-X-C motif chemokine 6	P80162	0.13 (0.02-0.24)	0.19 (0.08-0.30)
Trefoil factor 1	P04155	0.12 (0.03-0.21)	0.18 (0.11-0.25)
Programmed cell death protein 5	O14737	0.11 (0.00-0.22)	0.18 (0.09-0.27)
Cell surface A33 antigen	Q99795	0.19 (0.06-0.32)	0.18 (0.07-0.29)
Serine protease inhibitor Kazal-type 1	P00995	0.16 (0.10-0.23)*†	0.17 (0.12-0.22)
Regenerating islet-derived protein 3-alpha	Q06141	0.10 (0.02-0.17)	0.17 (0.10-0.23)
Promotilin	P12872	0.16 (0.08-0.25)*	0.17 (0.09-0.25)
Lithostathine-1-alpha	P05451	0.08 (0.01-0.16)	0.17 (0.09-0.24)
Proteinase-activated receptor 1	P25116	0.13 (0.03-0.23)	0.17 (0.08-0.26)
Acyl-CoA-binding protein	P07108	0.17 (0.05-0.28)	0.17 (0.07-0.26)
Kynurenine-oxoglutarate transaminase 1	Q16773	0.08 (-0.03 to 0.19)	0.17 (0.06-0.28)
NADH dehydrogenase [ubiquinone] iron-sulfur protein 6, mitochondrial	O75380	0.03 (-0.09 to 0.16)	0.17 (0.07-0.27)
Dickkopf-related protein 4	Q9UBT3	0.12 (0.05-0.18)	0.16 (0.10-0.23)
Guanylin	Q02747	0.17 (0.11-0.23)*†	0.16 (0.10-0.22)
Lymphocyte antigen 6D	Q14210	0.10 (0.04-0.16)	0.16 (0.10-0.21)
Adipocyte fatty acid-binding protein	P15090	0.17 (0.09-0.25)*†	0.16 (0.09-0.23)
Midkine	P21741	0.18 (0.09-0.27)*†	0.16 (0.09-0.23)
C-C motif chemokine 7	P80098	0.11 (0.04-0.18)	0.16 (0.09-0.23)
Stanniocalcin-1	P52823	0.11 (0.04-0.18)	0.16 (0.09-0.22)
Galectin-4	P56470	0.10 (0.03-0.18)	0.16 (0.09-0.22)
Renin	P00797	0.12 (0.02-0.22)	0.16 (0.07-0.25)
TP53-regulated inhibitor of apoptosis 1	O43715	0.04 (-0.06 to 0.4)	0.16 (0.07-0.25)
Matrix metalloproteinase-9	P14780	0.14 (0.03-0.24)	0.16 (0.07-0.26)
Phosphatidylethanolamine-binding protein 1	P30086	0.17 (0.05-0.29)	0.16 (0.07-0.25)
Copper transport protein ATOX1	O00244	0.10 (0.01-0.19)	0.16 (0.07-0.24)
2'-deoxynucleoside 5'-phosphate N-hydrolase 1	O43598	0.14 (0.03-0.25)	0.16 (0.06-0.26)
Stromal cell-derived factor 1	P48061	0.10 (0.04-0.15)	0.15 (0.10-0.21)
Angiopietin-related protein 4	Q9BY76	0.16 (0.09-0.22)*†	0.15 (0.09-0.21)
Calcitonin	P01258	0.10 (0.03-0.18)	0.15 (0.08-0.22)
Elafin	P19957	0.11 (0.04-0.18)*	0.15 (0.08-0.21)

Continued on the next page

TABLE 1 Continued

	UniProt ID	Log <sub>2</sub> Fold Change  (95% CI)	
		Discovery Cohort 1 (Olink 1536 Platform)	Validation Cohort 2 (Olink 3072 Platform)
Epithelial cell adhesion molecule	P16422	0.20 (0.10-0.29)*†	0.15 (0.07-0.23)
TNF ligand superfamily member 14	O43557	0.06 (-0.03 to 0.15)	0.15 (0.06-0.24)
C-C motif chemokine 22	O00626	0.12 (0.02-0.21)	0.15 (0.06-0.23)
26S proteasome non-ATPase regulatory subunit 9	O00233	0.12 (0.03-0.21)	0.15 (0.06-0.25)
Intercellular adhesion molecule 4	Q14773	0.13 (0.07-0.18)	0.14 (0.10-0.19)
Cerebral dopamine neurotrophic factor	Q49AHO	0.09 (0.04-0.14)	0.14 (0.09-0.19)
Insulin-like growth factor binding protein 4	P22692	0.17 (0.09-0.25)*†	0.14 (0.08-0.20)
Trefoil factor 2	Q03403	0.09 (0.01-0.17)	0.14 (0.07-0.21)
C-C motif chemokine 18	P55774	0.19 (0.10-0.28)*†	0.14 (0.06-0.22)
Follistatin	P19883	0.19 (0.12-0.26)*†	0.13 (0.07-0.20)
Cystatin-F	O76096	0.15 (0.06-0.24)*	0.13 (0.06-0.21)
Retinoic acid receptor responder protein 2	Q99969	0.17 (0.08-0.27)*†	0.13 (0.05-0.20)
Scavenger receptor cysteine-rich domain-containing group B protein	Q8WTU2	0.18 (0.09-0.27)*†	0.13 (0.05-0.20)
Phospholipase A2	P14555	0.16 (0.07-0.26)*	0.13 (0.04-0.22)
Neural proliferation differentiation and control protein 1	Q9NQX5	0.11 (0.06-0.17)*	0.12 (0.07-0.17)
Cystatin-M	Q15828	0.11 (0.05-0.17)*	0.12 (0.06-0.18)
C-C motif chemokine 16	O15467	0.13 (0.06-0.21)*	0.12 (0.05-0.18)
Connective tissue growth factor/nephroblastoma overexpressed family member 5	O76076	0.14 (0.07-0.21)*	0.11 (0.05-0.19)
C-C motif chemokine 27	Q9Y4X3	0.17 (0.07-0.27)*	0.11 (0.04-0.18)
Angiopoietin-related protein 2	Q9UKU9	0.14 (0.06-0.21)*	0.10 (0.03-0.17)
Beta-Ala-His dipeptidase	Q96KN2	0.19 (0.11-0.27)*†	0.06 (-0.01 to 0.14)
Osteopontin	P10451	0.13 (0.06-0.20)*	0.06 (-0.04 to 0.15)

There were 32 proteins that were identified as being differentially enriched in our discovery Cohort 1, based on a between-group difference  $\geq 10\%$  and a false discovery rate adjusted  $P$  value (FDR<sub>q</sub>)  $< 1\%$ , unadjusted for the change in estimated glomerular filtration rate (eGFR), as described in our original report.<sup>8</sup> \*These are designated above by an asterisk (\*). †However, when adjusted for changes in eGFR, 5 proteins with borderline values (cystatin-M, C-C motif chemokine 16, osteopontin, neural proliferation differentiation and control protein 1, and elafin) no longer showed a between-group difference of  $\geq 10\%$ , and additionally, only 16 proteins showed a  $\geq 10\%$  between-group difference and a FDR<sub>q</sub>  $< 1\%$ , adjusted for the change in eGFR; these are designated by a dagger (†). In the current validation Cohort 2, 117 proteins were identified to be differentially enriched, based on a between-group difference of  $\geq 10\%$  and a FDR<sub>q</sub>  $< 1\%$ , adjusted for the change in eGFR at 12 weeks; these are shown in Supplemental Table 2. Table 1 (above) lists the 72 proteins that fulfilled the definition of differential enrichment for Cohort 1 or for Cohort 2, as described above, and were measured in both cohorts. These 72 proteins exhibited a similar magnitude of differential enrichment in both cohorts; the estimates for only 3 proteins (mitochondrial ATPase inhibitor, retinol-binding protein 2, and C-C motif chemokine 28) differed by a |log<sub>2</sub> fold change| of at least 0.1375, corresponding to a  $\geq 10\%$  between-cohort difference. Proteins are ordered based on magnitude of differential enrichment in Cohort 2.

CEA = carcinoembryonic antigen; NADH = nicotinamide adenine dinucleotide; TNF = tumor necrosis factor.

Importantly, of these 16 proteins in our discovery Cohort 1, 12 proteins (75%) also showed a  $\geq 10\%$  between-group treatment effect (adjusted for the change in eGFR) and with FDR<sub>q</sub>  $< 1\%$  (FDR adjusted  $P < 0.01$ ), in our validation Cohort 2 (Table 1).

To further elucidate the assay reproducibility across the 2 platforms, we examined the concordance for the 72 proteins that fulfilled our definition of differential enrichment in our original discovery Cohort 1<sup>8</sup> or in our validation Cohort 2, and were measured both in cohorts (Table 1). In general, these 72 proteins exhibited a similar magnitude of differential enrichment in both cohorts; the estimates for only 3 proteins (4%)—mitochondrial ATPase inhibitor (ATPFI), retinol-binding protein 2 and C-C motif chemokine 28—differed by a |log<sub>2</sub> fold change| of at least 0.1375, corresponding to an

absolute  $\geq 10\%$  difference between our discovery and validation cohorts.

**Proteins showing between-group difference  $\geq 15\%$  with FDR<sub>q</sub>  $< 1\%$  at 12 weeks.** Because of the shedding and secretion of proteins varies and stoichiometric relationships are not known, the selection of a threshold difference is arbitrary, and thus we also explored a  $\geq 15\%$  between-group difference with a FDR<sub>q</sub>  $< 1\%$  (FDR-adjusted  $P < 0.01$ ) at 12 weeks in our original discovery Cohort 1.<sup>8</sup> In Cohort 1, using the limited Olink Explore 1536 platform, only 9 proteins had exhibited a  $\geq 15\%$  between-group increase with a FDR<sub>q</sub>  $< 1\%$ , and only 3 proteins exhibited a  $\geq 15\%$  between-group increase with a FDR<sub>q</sub>  $< 1\%$  after adjustment for the change in eGFR.<sup>8</sup>

By contrast, in our current validation Cohort 2, 28 proteins showed a  $\geq 15\%$  between-group increase at

**TABLE 2** Differentially Enriched Proteins at 12 Weeks,  $\geq 15\%$  Between-Group Difference With FDRq  $< 1\%$ , Adjusted for Change in eGFR at 12 Weeks (Validation Cohort 2)

Protein	UniProt ID	Empagliflozin vs Placebo [log <sub>2</sub> fold change (95% CI)]	False Discovery Rate (%)
Alpha-synuclein	P37840	0.45 (0.21, 0.69)	0.20
Mitochondrial ATPase inhibitor	Q9UII2	0.31 (0.13, 0.49)	0.60
Retinol-binding protein 2	P50120	0.30 (0.21, 0.39)	<0.01
IST1 homolog associated with ESCRT-III	P53990	0.28 (0.11, 0.45)	0.70
Tubulin-specific chaperone A	O75347	0.27 (0.12, 0.42)	0.47
DnaJ homolog subfamily C member 9	Q8WXX5	0.26 (0.11, 0.41)	0.58
Cystatin-SN	P01037	0.26 (0.16, 0.36)	<0.01
DnaJ homolog subfamily B member 1	P25685	0.26 (0.10, 0.42)	0.98
C-C motif chemokine 5	P13501	0.25 (0.10, 0.41)	0.85
Fatty acid-binding protein, liver	P07148	0.25 (0.14, 0.36)	0.03
Creatine kinase U-type, mitochondrial	P12532	0.25 (0.12, 0.37)	0.13
Ubiquitin thioesterase OTU1	Q5VVQ6	0.24 (0.12, 0.36)	0.18
Uncharacterized protein C9orf40	Q8IXQ3	0.24 (0.11, 0.38)	0.38
C-C motif chemokine 28	Q9NRJ3	0.23 (0.14, 0.33)	0.01
Chromogranin-A	P10645	0.23 (0.13, 0.34)	0.04
Acylphosphatase-1	P07311	0.23 (0.11, 0.35)	0.17
Hsc70-interacting protein	P50502	0.23 (0.11, 0.35)	0.19
Fatty acid-binding protein, heart	P05413	0.23 (0.15, 0.31)	0.01
Fatty acid-binding protein 5	Q01469	0.23 (0.12, 0.33)	0.04
Insulin-like growth factor-binding protein 1	P08833	0.22 (0.09, 0.36)	0.83
Carbonic anhydrase 2	P00918	0.22 (0.09, 0.35)	0.65
Immunoglobulin-binding protein 1	P78318	0.22 (0.10, 0.34)	0.39
Transferrin receptor protein 1	P02786	0.22 (0.16, 0.28)	<0.01
Myeloid-derived growth factor	Q969H8	0.22 (0.09, 0.35)	0.71
Erythroid membrane-associated protein	Q96PL5	0.21 (0.15, 0.28)	<0.01
Erythropoietin	P01588	0.21 (0.09, 0.33)	0.33
Uroporphyrinogen decarboxylase	P06132	0.21 (0.08, 0.34)	0.84
Gastrotropin	P51161	0.21 (0.12, 0.29)	0.01

12 weeks with a FDRq  $< 1\%$  adjusted for the change in eGFR (Table 2), and, of these 28 proteins, 15 (54%) proteins had not been measured in our discovery Cohort 1. All 3 proteins that showed a between-group difference  $\geq 15\%$  with a FDRq  $< 1\%$  (adjusted for the change in eGFR) in our discovery Cohort 1 fulfilled these same criteria in our validation Cohort 2. These proteins were mitochondrial creatine kinase U-type, insulin-like growth factor binding protein 1, and transferrin receptor protein 1.

**Proteins showing between-group difference  $\geq 10\%$  with FDRq  $< 1\%$  at 52 weeks.** In the validation Cohort 2, the changes seen at 52 weeks were generally consistent with those observed at 12 weeks (all treatment-by-visit interaction FDRq  $> 1\%$ ; FDR-adjusted  $P > 0.01$ ), although  $\approx 40\%$  of cohort participants did not provide paired data at 52 weeks, and—in general—the magnitude of the between-group differences became smaller after 1 year. In our discovery cohort, we observed a between-visit interaction only for kidney injury molecule 1,<sup>8</sup> but this was not confirmed in the validation Cohort 2. In validation Cohort 2, 2 proteins fulfilled criteria for between-group differential

enrichment at the  $\geq 10\%$  threshold at 52 weeks: uromodulin (11% increase, FDRq = 0.08%) and cadherin-related family member 2 (11% decrease, FDRq = 0.35%).

**BIOLOGICAL ACTIONS OF DIFFERENTIALLY ENRICHED PROTEINS.** To elucidate the biological profile of differentially enriched proteins, we performed an exhaustive PubMed-based individual documentation of the described cardiac and renal actions of each protein in lieu of the conventional algorithm-driven ontology classification based on oncology pathway-based assumptions. We had used this same approach to describe the action of differentially-enriched proteins in discovery Cohort 1.<sup>8</sup> To allow for a thorough characterization of the biological effects of a reasonable number of proteins in our validation Cohort 2, we initially focused on the 30 proteins that showed a  $\geq 15\%$  between-group difference with a FDRq  $< 1\%$  at 12 weeks or a  $\geq 10\%$  between-group difference with a FDRq  $< 1\%$  at 52 weeks, both adjusted for the change in eGFR (Table 3).

Of these 30 proteins, 25 proteins have functions in the heart and kidney.<sup>11-93</sup> Table 3 allocates these

**TABLE 3 Biological Functions of Differentially-Enriched Proteins ( $\geq 15\%$  Between-Group Difference at 12 Weeks With FDRq  $< 1\%$  or  $\geq 10\%$  Between-Group Difference at 52 Weeks With FDRq  $< 1\%$ ) With Reported Effects on the Heart and Kidneys (Validation Cohort 2)**

Protein	Cellular Effects	Effect on the Heart or Kidneys
Promotion of Autophagy and Cellular Quality Control in Heart and Kidney		
Insulin-like growth factor-binding protein 1 (IGFBP1)	IGFBP1 binds to and inhibits effect of insulin-like growth factor 1 (IGF1).	IGF1 promotes heart failure and chronic kidney disease by inhibiting autophagy. <sup>11</sup> Increases in IGFBP1 interfere with actions of IGF1, thus promoting autophagy. IGFBP1 also directly inhibits cardiomyocyte and renal tubular apoptosis. <sup>12,13</sup>
IST1 factor associated with endosomal sorting complex required for transport component III (ESCRT-III) [IST1 homolog]	ESCRT-III binds to ubiquitinated injured organelles to deliver them to lysosomes and thus promote clearance by autophagy.	When stimulated by Beclin-1, it binds to damaged mitochondria to promote clearance by mitophagy. Suppression of ESCRT-III leads to accumulation of stressed mitochondria, apoptosis of cardiomyocytes, and cardiomyopathy. <sup>14-16</sup> ESCRT mediates fatty acid transfer into mitochondria. <sup>17</sup> ESCRT-III-mediated endocytosis regulates ion transport channels in the renal tubules. <sup>18</sup>
OTU domain-containing ubiquitin aldehyde-binding protein 1 (OTUB1)	OTUB1 is a hydrolase that removes conjugated ubiquitin from proteins, thereby preventing degradation.	Deubiquitination by OTUB1 suppresses Akt-mTOR signaling, thereby enhancing autophagy and energy metabolism. <sup>19,20</sup> OTUB1 attenuates development of diabetic cardiomyopathy and renal ischemia-reperfusion injury. <sup>21,22</sup>
Heat shock cognate 70-interacting protein (HSPA8, CHIP, Stub1)	The carboxy terminus of HSPA8 is a U-box E3 ubiquitin ligase, which plays a crucial role in protein quality control by regulating chaperone-mediated autophagy and mitophagy. <sup>23</sup>	HSPA8 activates AMPK and autophagic flux to prevent inflammation, fibrosis, apoptosis, and pathologic hypertrophy in infarction and pressure overload models. <sup>24-26</sup> It exerts nephroprotective effects by preventing renal tubular pyroptosis and ferroptosis <sup>27,28</sup> and mediates transfer of enzymes into mitochondria for generation of energy. <sup>29</sup>
DnaJ homolog subfamily B member 1 (DNAJB1)	Molecular chaperone stimulates the ATPase activity of heat shock protein 70 to prevent aggregation and to enhance clearance of misfolded proteins through promotion of chaperone-mediated autophagy. <sup>30</sup>	Generally assumed that upregulation of DNAJB1 is an adaptive response; upregulated in cardiomyocytes in response to anticancer proteasome inhibitors <sup>31</sup> and in the kidney in hypertensive nephropathy. <sup>32</sup>
DnaJ homolog subfamily C member 9 (DNAJC9)	Molecular chaperone stimulates the ATPase activity of heat shock protein 70 to prevent misfolded histones to maintain chromatin integrity. <sup>33,34</sup>	Generally assumed that upregulation of DNAJC9 is an adaptive response; upregulated in experimental pulmonary hypertension with normalization following carvedilol treatment. <sup>35</sup>
Immunoglobulin-binding protein 1 ( $\alpha 4$ subunit of protein phosphatase 2A [Pp2a], IGBP1)	IGBP1 protects phosphatase Pp2a, thereby promoting autophagy and preventing apoptosis in a broad range of tissues.	Pp2a promotes autophagic clearance of damaged mitochondria in renal tubules. <sup>36</sup> Dephosphorylating action mediates its effects to attenuate ventricular hypertrophy. <sup>37,38</sup> It is an erythropoietin-responsive protein that promotes erythroblast proliferation. <sup>39</sup>

Continued on the next page

proteins into categories based on their primary cardiac or renal action, recognizing that these groupings may overlap. These categories include: 1) proteins involved in autophagic cellular quality control: that is, insulin-like growth factor-binding protein 1 (IGFBP1), endosomal sorting complex required for transport component III (ESCRT-III), ovarian tumor domain-containing ubiquitin aldehyde-binding protein 1 (OTUB1), heat shock cognate 70-interacting protein 8 (HSPA8), DnaJ homolog subfamily B member 1 (DNAJB1), DnaJ homolog subfamily C member 9 (DNAJC9), and immunoglobulin-binding protein 1 (IGBP1); 2) proteins involved in mitochondrial energy homeostasis: that is, mitochondrial creatine kinase U-type (uMtCK), tubulin-specific chaperone A (TBCA), mitochondrial ATPase inhibitor (ATPIF1), liver fatty acid-binding protein (L-FABP [also known as FABP1]), heart fatty acid-binding protein (H-FABP [also known as FABP3]), fatty acid-binding protein 5 (FABP5), fatty

acid-binding protein 6 (FABP6), and retinol-binding protein 2 (RBP2); 3) proteins involved in augmented iron mobilization and erythropoiesis: that is, transferrin receptor protein 1 (TfR1), erythropoietin (EPO), erythroid membrane-associated protein (ERMAP), uroporphyrinogen decarboxylase (UROD), and alpha-synuclein (SNCA); 4) proteins that mediate ion (primarily sodium) reabsorptive responses in renal tubules: that is, uromodulin (UMOD), carbonic anhydrase 2 (CA2) and acylphosphatase-1 (ACYP1); and 5) proteins that exert other restorative effects on cardiac structure and function: myeloid-derived growth factor (MYDGF) and chromogranin-A (CgA).

When overlap functions are considered, of the 25 differentially-enriched proteins with effects on the heart and kidney, it is noteworthy that: 1) 13 proteins promote autophagy or other cellular quality control functions (IGFBP1, OTUB1, DNAJB1, DNAJC9, RBP2, ESCRT-III, HSPA8, H-FABP, FABP6, ATPIF1, TfR1,

TABLE 3 Continued

Protein	Cellular Effects	Effect on the Heart or Kidneys
<b>Restoration of Mitochondrial Energy Homeostasis</b>		
Mitochondrial creatine kinase U-type (uMtCK)	uMtCK couples ATP production via oxidative phosphorylation to phosphocreatine in the cytosol.	uMtCK mediates the transfer of high energy phosphate from mitochondria to cytosol. Compensatory increase following oxidative stress exerts cardioprotective effects <sup>40,41</sup> and contributes to energy homeostasis in the renal tubules. <sup>42</sup>
Tubulin-specific chaperone A (TBCA)	TBCA facilitates assembly of $\beta$ -tubulin cytoskeletal protein, which (in conjunction with uMtCK) determines mitochondrial stability and efficient energy transfer. <sup>43,44</sup>	$\beta$ -tubulin interactions with mitochondria are disrupted in cardiac ischemia-reperfusion injury and volume overload, contributing to loss of ATP homeostasis. <sup>45,46</sup>
Mitochondrial ATPase inhibitor (ATPIFI)	ATPIFI prevents wasteful hydrolysis of ATP. <sup>47</sup> It promotes mitophagy and healthy mitochondrial function. <sup>48</sup>	ATPIFI acts to preserve ATP and myocardial function during ischemia. <sup>47</sup> It is essential for heme synthesis and maturation of erythroblasts. <sup>49</sup> Silencing or overexpression of ATPIFI impairs cardiac adaptation to stress.
Liver fatty acid-binding protein (L-FABP, FABP1)	Transports long-chain fatty acids from cell membrane to mitochondria. Activated by PPAR- $\alpha$ signaling.	Effect on the heart and kidneys has not been elucidated.
Heart fatty acid-binding protein (H-FABP, FABP3)	Transports long-chain fatty acids from cell membrane to mitochondria. Activated by PPAR- $\alpha$ signaling.	Enhances uptake and use of long-chain fatty acids by cardiomyocytes. <sup>50</sup> Binds acylcarnitines, the deleterious lipid byproduct that is injurious to mitochondria. <sup>51</sup> Deficiency of H-FABP leads to toxic lipid accumulation and compromises fatty acid oxidation and ATP production. <sup>50,51</sup> Also acts as autophagy receptor substrate. <sup>52</sup>
Fatty acid-binding protein 5 (FABP5)	Transports long-chain fatty acids from cell membrane to mitochondria. Activated by PPAR- $\alpha$ signaling.	Enhances uptake and use of long-chain fatty acids. FABP5 deficiency aggravates cardiac hypertrophy, fibrosis, and dysfunction, and it causes severe impairment to mitochondria in the heart with increased oxidative stress and reduced mitochondrial respiration. <sup>53</sup>
Gastrotrypin, fatty acid binding protein 6 (FABP6)	Transports long-chain fatty acids from cell membrane to mitochondria. Activated by PPAR- $\alpha$ signaling. Promotes autophagic flux. <sup>54</sup>	FABP6 expression increased in cardiomyocytes under stress. <sup>55</sup>
Retinol-binding protein 2 (RBP2)	Member of fatty acid-binding protein family, which coordinates transport of retinol, primarily in gastrointestinal tract	Retinoic acid levels decline in heart failure. <sup>56</sup> RBP2 facilitates dietary uptake of retinols, thereby promoting cardiomyocyte mitophagy and mitigating cardiomyocyte apoptosis. <sup>57,58</sup> Retinols prevent renal injury by promoting autophagy. <sup>59</sup>
<b>Effects on Iron Metabolism and Erythropoiesis</b>		
Transferrin receptor protein 1 (TfR1)	TfR1 promotes uptake of iron into cardiomyocytes (for ATP production) and erythroblasts (for erythropoiesis). Enhances the transmembrane electron transport needed for sirtuin-1 upregulation.	TfR1 knockout leads to mitochondrial dysfunction, downregulation of cardiac autophagy proteins and cardiomyopathy, which can be prevented by sirtuin-1 activation. <sup>60</sup> TfR1 provides NAD <sup>+</sup> , which is needed for sirtuin activation and mitochondrial health. <sup>61</sup>
Erythropoietin (EPO)	EPO is the primary stimulus for erythropoiesis. EPO also acts directly on the heart and kidneys to exert cytoprotective effects, mediated by AMPK and sirtuin 1. <sup>6</sup>	EPO acts to promote autophagy and mitigate mitochondrial ATP depletion, apoptosis, inflammation, fibrosis, and adverse remodeling in the heart. <sup>62,63</sup> EPO is a downstream effector of Klotho-induced renal cytoprotection, reducing oxidative stress in renal tubules. <sup>64,65</sup>
Erythroid membrane-associated protein (ERMAP)	Cell-surface protein is expressed almost exclusively in erythroid precursor cells and expressed during enhanced erythropoiesis. <sup>66</sup>	Effect on the heart and kidneys has not been elucidated.
Uroporphyrinogen decarboxylase (UROD)	Ferrous iron-inducible enzyme, essential for synthesis of heme. <sup>67,68</sup>	Suppression is associated with increase in oxidative stress in the kidney. <sup>69</sup>
Alpha-synuclein (SNCA)	Iron provokes oligomerization of alpha-synuclein, binding to peroxidized lipids to cause iron-dependent mitochondrial dysfunction and synchronized cell death. <sup>70</sup>	SNCA has been implicated in development and progression of ferroptosis-mediated cardiomyopathy. <sup>71</sup> Conversely, it may interfere with PI3K-Akt signaling to prevent renal fibrosis. <sup>72</sup>
<b>Restorative Effects on Cardiac and Renal Structure and Function</b>		
Myeloid-derived growth factor (MYDGF)	Produced by monocytes and macrophages, MYDGF mediates crosstalk between bone marrow and the heart.	MYDGF inhibits cardiac hypertrophy and augments SERCA2a to attenuate pressure-overload induced heart failure. <sup>73</sup> Induces cardiomyocyte proliferation to improve postinfarction cardiac function. <sup>74,75</sup> Silencing and upregulation modulate exacerbates podocyte survival in nephropathy. <sup>76,77</sup>
Chromogranin-A (CgA)	CgA is secreted in cardiac neuroendocrine granules to limit effects of sympathetic overactivity. <sup>78,79</sup> CgA is a precursor to catestatin, which exerts cardioprotective effects. <sup>80</sup>	Chromogranin-A and catestatin reduces mitochondrial generation of reactive oxygen species, attenuates hypertrophy, and prevents apoptosis in cardiomyocytes under stress. <sup>78-80</sup> May mediate antihypertensive effects of drugs. <sup>81</sup>

Continued on the next page

TABLE 3 Continued

Protein	Cellular Effects	Effect on the Heart or Kidneys
Counter-Regulatory Sodium Reabsorption in the Renal Tubules		
Acylphosphatase-1 (ACYPI)	ACYPI enhances activity of renal tubular Na <sup>+</sup> -K <sup>+</sup> -ATPase. <sup>82</sup> It also hydrolyzes the phosphoenzyme intermediate of SERCA2a, displacing phospholamdan, thus enhancing activity of sarcoplasmic reticulum Ca <sup>2+</sup> pump. <sup>83</sup>	Effect of ACYPI to stimulate renal tubular Na <sup>+</sup> -K <sup>+</sup> -ATPase promotes sodium reabsorption as a counterregulatory response to the action of SGLT2 inhibitors in the proximal renal tubule. <sup>84</sup> Effect of ACYPI on SERCA2a leads to enhanced cardiac contractility. <sup>85</sup>
Uromodulin (UMOD)	UMOD is a major regulator renal tubular sodium transport, and it acts to suppress renal inflammation.	UMOD promotes sodium reabsorption in the thick ascending limb of the loop of Henle. <sup>86</sup> Acts as a trap for proinflammatory renal cytokines; loss-of-function mutations lead to mitochondrial dysfunction and chronic kidney disease. <sup>87,88</sup>
Carbonic anhydrase 2 (CA2)	CA2 is a major regulator of renal tubular sodium, bicarbonate, and water homeostasis.	CA2 binds to and enhances the activity of NHE3 in the proximal renal tubule. <sup>89</sup> CA2 may offset increases in urinary excretion of sodium and bicarbonate resulting from SGLT2 inhibition.
Other Differentially Expressed Proteins		
Cystatin-SN (CST1)	Cysteine protease inhibitor involved in regulation of cellular proliferation	Effect on the heart and kidneys has not been elucidated.
C-C motif chemokine 5 (CCL5, RANTES)	Proinflammatory cytokine acting through PI3K-Akt signaling; it is also a negative regulator of GPR75, the receptor for the vasoconstrictor, 20-hydroxyeicosatetraenoic acid.	CCL5 upregulation increases infarct size and promotes heart failure following myocardial infarction. <sup>90</sup> CCL5-mediated negative regulation of GPR75 function acts to ameliorate obesity and hypertension. <sup>91</sup>
C-C motif chemokine 28 (CCL28)	CCL28 interacts with its receptor CCR10 to promote inflammation in epithelial cells and inhibit angiogenesis. <sup>92</sup>	Effect on the heart and kidneys has not been elucidated.
Cadherin-related family member 2 (CDHR2)	Calcium-dependent cell-cell adhesion molecule is localized at the distal ends of microvilli, where it forms an intermicrovillar adhesion complex. <sup>93</sup>	Effect on the heart and kidneys has not been elucidated.
A total of 30 proteins showed a $\geq 15\%$ between-group difference with a FDRq $< 1\%$ at 12 weeks or a $\geq 10\%$ between-group difference with a FDRq $< 1\%$ at 52 weeks, both adjusted for the change in eGFR. "Uncharacterized protein C9orf40" is not included in this listing, and thus the Table describes 29 proteins.		
Akt = protein kinase B; AMPK = adenosine monophosphate protein kinase; ATP = adenosine triphosphate; CHIP = carboxy terminus of Hsp70-interacting protein HSPA8, acting as E3 ubiquitin-protein ligase (Stub1 as gene designation); CCL5 = regulated on activation, normal T cell expressed and secreted, also known as C-C motif chemokine 5; CCL28 = C-C motif chemokine 28; CCR10 = C-C motif chemokine receptor 10; CST1 = cystatin-SN; GPR75 = global and endothelial G-protein coupled receptor 75; NAD = nicotinamide adenine dinucleotide; NHE3 = sodium-hydrogen exchanger 3; PI3K = phosphoinositide-3-kinase; Pp2a = $\alpha$ subunit of protein phosphatase 2A; PPAR- $\alpha$ = peroxisome proliferator-activated receptor- $\alpha$ ; mTOR = mammalian target of rapamycin; RANTES = regulated on activation, normal T cell expressed and secreted, also known as C-C motif chemokine 5; SERCA2a = sarcoplasmic/endoplasmic reticulum Ca <sup>2+</sup> -ATPase-2a.		

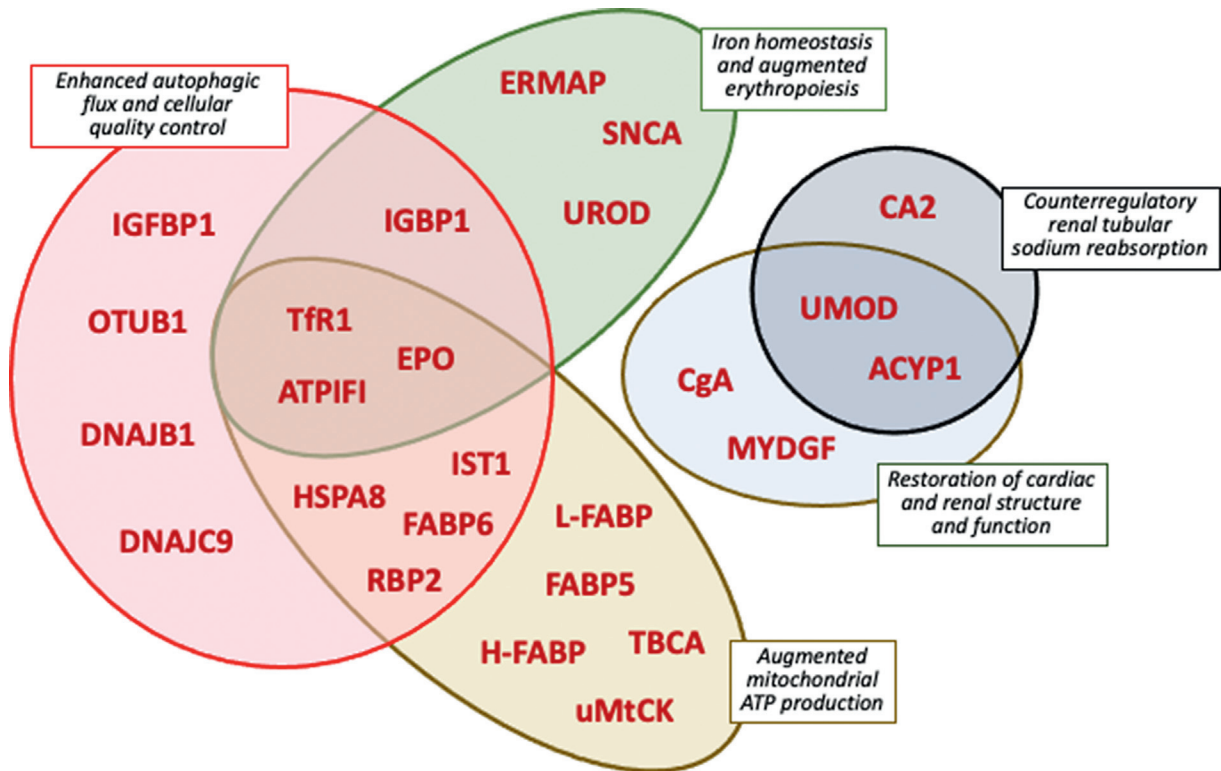
EPO, IGBP1); 2) 12 proteins enhance mitochondrial health and ATP production directly or by promoting substrate use (UMtCK, TBCA, L-FABP, H-FABP, FABP5, FABP6, RBP2, ESCRT-III, HSPA8, ATP1F1, TfR1, EPO); 3) 7 proteins augment iron mobilization or erythropoiesis (TfR1, EPO, IGBP1, ERMAP, UROD, ATP1F1, SNCA); 4) 3 proteins influence renal tubular sodium handling (UMOD, CA2, and ACYP1); and 5) 9 proteins mitigate injury and have restorative effects in the heart or kidneys (IGFBP1, OTUB1, HSPA8, IGBP1, EPO, MYDGF, UMOD, CgA, and ACYP1). These biological functional intersections are shown in [Figure 1](#).

To determine if our selection of a  $\geq 15\%$  between-group difference threshold influenced the characterization of the proteomic signatures of SGLT2 inhibition, we examined the biological effects of differentially enriched proteins with a between-group difference: that is,  $\geq 10\%$  but  $< 15\%$  increase  $|\log_2$  fold change| of  $> 0.1375$  and  $< 0.2016$  with empagliflozin (adjusted for the change in eGFR) and with a FDRq  $< 1\%$ ; we had also used this threshold in our

original discovery cohort.<sup>8</sup> Of the 58 proteins showing a between-group difference within this range and having demonstrated effects on the heart or kidneys ([Supplemental Table 3](#)), 18 proteins are known to promote cargo targeting, autophagic flux, and cellular quality control; 6 proteins enhance mitochondrial health and production of ATP; 32 proteins are involved in the modulation of cardiac and renal structure and function; 5 proteins exert effects on renal tubular ion transport; and 7 proteins contribute to or reflect enhanced iron mobilization and erythropoiesis, with many proteins exerting more than 1 function. This pattern closely resembled the mechanistic signatures of the differentially enriched proteins that showed a  $\geq 15\%$  between-group difference ([Table 3](#)).

## DISCUSSION

Many studies have reported on the effect of a broad range of treatments on circulating levels of proteins in patients with heart failure, with results that

**FIGURE 1** Mechanistic Categorization of Most Differentially Expressed Proteins With Known Effects on the Heart and Kidneys

These proteins showed a  $\geq 15\%$  between-group increase at 12 weeks with a FDRq  $< 1\%$  adjusted for the change in eGFR or  $\geq 10\%$  between-group increase at 52 weeks with a FDRq  $< 1\%$  adjusted for the change in eGFR and had known effects on the heart and kidney. Effects on autophagic flux and mitochondrial health and ATP production reflect the findings of studies in the heart or kidney. Effects on iron homeostasis reflect the findings of studies in the bone marrow or heart. Proteins exerting effects in more than 1 domain are shown in areas of overlap. ACYP1 = acylphosphatase-1; ATP = adenosine triphosphate; ATPIFI = mitochondrial ATPase inhibitor; CA2 = carbonic anhydrase 2; CgA = chromogranin-A; DNAJB1 = DnaJ homolog subfamily B member 1; DNAJC9 = DnaJ homolog subfamily C member 9; eGFR = estimated glomerular filtration rate; EPO = erythropoietin; ERMAP = erythroid membrane-associated protein; ESCRT-III = endosomal sorting complex required for transport component III; FABP5 = fatty acid-binding protein 5; FABP6 = fatty acid-binding protein 6; IGFBP1 = insulin-like growth factor-binding protein 1H; H-FABP = heart fatty acid-binding protein; HSPA8 = heat shock cognate 70-interacting protein; IGFBP1 = immunoglobulin-binding protein 1; IST1 = increased sodium tolerance homolog 1 associated with endosomal sorting complex required for transport component III; L-FABP = liver fatty acid-binding protein; MYDGF = myeloid-derived growth factor; OTUB1 = OTU domain-containing ubiquitin aldehyde-binding protein 1; RBP2 = retinol-binding protein 2; SNCA = alpha-synuclein; TBCA = tubulin-specific chaperone A; TfR1 = transferrin receptor protein 1; UMOD = uromodulin; uMtCK = mitochondrial creatine kinase U-type; UROD = uroporphyrinogen decarboxylase.

typically show little consistency across reports. The lack of consistency can be explained by differences in patient populations, sample size, and analytic technologies; in the number and identity of the proteins being measured; and in the lack of a placebo-control group. Furthermore, most previous studies of proteomics in heart failure have applied commercially available algorithms to characterize the biological actions of proteins, but most proteins have pleiotropic effects, and current interpretative ontology programs rely primarily on the assessment of the effect of a protein in experimental models of cancer or neurologic disorders but not in models of

cardiovascular or kidney disease. Most importantly, no previous study has measured a large set of proteins using the same analytic methodology, in both a discovery and validation cohort derived from a common group of patients, to determine if the principal conclusions concerning the mechanisms of action of a drug based on the discovery cohort could be verified.

We evaluated the effect of the SGLT2 inhibitor empagliflozin on a large number of blood-borne proteins in  $> 2,200$  patients enrolled in the EMPEROR trial program. Patients were randomly assigned to treatment with placebo or empagliflozin, and hence we could measure baseline-anchored between-group

differences in an unbiased and blinded manner. We had previously reported our findings of 1,283 proteins analyzed in a discovery cohort of 1,134 patients enrolled in the EMPEROR program, and herein we analyzed 2,155 proteins in a validation cohort of 1,120 different EMPEROR program participants who had not been included in the earlier cohort. In both cohorts, we measured an overlapping set of proteins using the same technology; we performed measurements at the same time points; we used similar statistical methods and thresholds to identify differentially enriched proteins; and we interpreted our findings based on biological effects and ontologic categories that were relevant to cardiovascular and renal disease. These features represent a unique set of conditions that provide an unprecedented level of robustness to our results.

The magnitude of the degree of differential enrichment in proteins as a result of treatment with empagliflozin was generally similar in the discovery and validation cohorts (Table 2). More importantly, the biological signatures of the differentially enriched proteins identified in the discovery Cohort 1 were reproduced in the validation Cohort 2 based on a much larger number of proteins (Table 3, Supplemental Table 3). The robust replication of these mechanistic signatures across the discovery and validation cohorts is closely aligned with the demonstrated cellular and organ effects of SGLT2 inhibitors that have been consistently reported in numerous experimental studies.<sup>2,4,6</sup>

SGLT2 inhibitors induce a state of starvation mimicry characterized clinically by gluconeogenesis and ketogenesis and experimentally by the upregulation of nutrient deprivation signaling pathways, which stimulate an evolutionarily-conserved starvation-induced housekeeping function, autophagy.<sup>2-4</sup> The self-digestion of unwanted cellular constituents not only generates ATP but also clears the cell of deleterious injured organelles (especially mitochondria, peroxisome, and endoplasmic reticulum), which are the primary source of oxidative stress and proinflammatory and profibrotic signaling.<sup>2,3</sup> Autophagy is suppressed, and cellular stress is markedly increased in the failing heart and in chronic kidney disease.<sup>2,4</sup> Experimentally, SGLT2 inhibitors have been shown to promote autophagic flux, thereby reducing oxidative stress and apoptosis, both in the heart and kidneys, and—importantly—silencing of nutrient deprivation and autophagic proteins blocks the cardioprotective effects of these drugs.<sup>2</sup> It is therefore noteworthy that 13 of the 30 differentially enriched proteins (based on  $\geq 15\%$  between-group difference) in validation Cohort 2 play a role in promoting

autophagy and other cellular quality control functions (Table 3). In our earlier report of discovery Cohort 1,<sup>8</sup> we highlighted the SGLT2 inhibitor-mediated enrichment of IGFBP1, erythropoietin, TfR1, and RBP2 as autophagy-enhancing proteins. In the current analysis in validation Cohort 2, we confirmed the differential upregulation of these 4 proteins, and we identified the differential enrichment of 9 additional autophagy-enhancing proteins (based on a  $\geq 15\%$  between-group difference), most of which were not available for assay in the Olink Explore 1536 platform used for discovery Cohort 1. These include IST1 and OTUB1, which regulate ubiquitination, a mechanism that marks injurious cellular constituents for autophagic lysosomal disposal.<sup>17-22</sup> In addition, HSPA8, DNAJB1, and DNAJC9 specifically mediate chaperone-mediated autophagy (which is responsible for the clearance of misfolded proteins and histone-targeted fragments of chromatin);<sup>23-26</sup> ATPIFI1 and IGBP1 promote mitophagy (the clearance of dysfunctional mitochondria)<sup>36,47-49</sup>; and H-FABP and FABP6 can act as an autophagy substrate or influence the degradation of autophagosomes.<sup>52,54</sup> As a result of autophagy upregulation, these 9 proteins have been shown to improve cardiac and renal structure and function (Table 3). Importantly, an additional 18 proteins with a FDRq <1% but with a  $\geq 10\%$  but <15% between-group difference in validation Cohort 2 are also involved in cargo targeting and autophagy modulation (Supplemental Table 3). Of note, 3 of these 18 proteins—acyl-CoA-binding protein, adipocyte fatty acid-binding protein, and mitochondrial import receptor subunit TOM20 homolog—have been proposed as blood-borne biomarkers of enhanced intracellular autophagic flux.<sup>94-96</sup>

Experimentally, the ability of the failing heart and stressed proximal renal tubular cells to generate ATP is impaired: in part related to dysfunctional mitochondria and in part related to a shift in metabolism from long-chain fatty acids to glycolysis.<sup>4</sup> SGLT2 inhibitors restore ability of these high oxygen-consuming cells to generate ATP by enhancing intracellular fatty acid transport and oxidation and by restoring mitochondrial health as a result of the increased disposal of injured mitochondria and the augmentation of healthy mitochondrial biogenesis.<sup>2,4</sup> We previously identified upregulation of uMtCK and other proteins involved in mitochondrial health in our discovery Cohort 1,<sup>8</sup> and in our validation Cohort 2, we identified 8 additional differentially enriched proteins (based on a  $\geq 15\%$  between-group difference)—not measured in Cohort 1—that support this important role. The 12 proteins involved in mitochondrial energy generation included 6 lipid-binding

and transit proteins (L-FABP, H-FABP, FABP5, FABP6, RBP2, and ESCRT-III), which facilitate the delivery of long-chain fatty acids to the mitochondria for oxidative phosphorylation. In addition, the upregulation of TBCA facilitates the assembly of cytoskeleton structures that are required for efficient energy transfer;<sup>45,46</sup> HSPA8 mediates transport of enzymes into mitochondria;<sup>29</sup> uMtCK promotes the transfer of synthesized ATP from mitochondria into the cytosol;<sup>41,42</sup> ATP1F1 prevents the wasteful hydrolysis of ATP;<sup>47</sup> and EPO and TfR1 promote mitochondrial health and biogenesis, thus preventing mitochondrial ATP depletion.<sup>60-63</sup> Importantly, an additional 6 proteins with a FDRq <1% but with a  $\geq 10\%$  but <15% between-group difference in validation Cohort 2 are also involved in sustaining mitochondrial health and ATP synthesis (Supplemental Table 3).

A characteristic feature of SGLT2 inhibitors is their action to increase hemoglobin and hematocrit because of augmented erythropoiesis.<sup>6</sup> These drugs simultaneously increase the production of erythropoietin and enhance the mobilization of iron from macrophages and intracellular stores (caused by the suppression of hepcidin and ferritin), thereby increasing cytosolic levels of the highly reactive ferrous iron required for the synthesis of heme and iron-sulfur clusters.<sup>4,6</sup> We previously reported increases in EPO and TfR1 in our discovery Cohort 1, and their upregulation was confirmed in our validation Cohort 2. Moreover, in Cohort 2, we found differential enrichment of 5 additional proteins (based on a  $\geq 15\%$  between-group difference)—IGBP1, ERMAP, UROD, ATP1F1, and SNCA—involved in enhanced iron mobilization and erythropoiesis; these proteins had not been measured in Cohort 1. UROD is induced by iron and essential to the synthesis of heme;<sup>67,68</sup> IGBP1 prolongs the proliferation of erythroblasts;<sup>39</sup> ATP1F1 promotes heme synthesis and erythroblast maturation;<sup>49</sup> ERMAP is an erythrocyte membrane constituent and a marker of enhanced erythropoiesis;<sup>66</sup> and  $\alpha$ -synuclein (SNCA) promotes ferroptosis, which occurs during intense repletion of reactive ferrous iron in the cytosol.<sup>70</sup> The action of  $\alpha$ -synuclein on ferroptosis is believed to mediate its neurotoxic effects in Parkinson disease,<sup>97</sup> but it has been proposed that other neuroprotective actions of SGLT2 inhibitors may counter this effect.<sup>98</sup> Interestingly, an additional 7 proteins with a FDRq <1% but with a  $\geq 10\%$  but <15% between-group difference in validation Cohort 2 have been implicated in augmented iron mobilization and erythropoiesis (Supplemental Table 3).

SGLT2 inhibitors exert natriuretic and diuretic effects whose duration is short-lived, because of the activation of distal-nephron counterregulatory

mechanisms that promote sodium reabsorption.<sup>5</sup> In our discovery Cohort 1, we identified CA2 and UMOD as potential mediators of this enhanced sodium reabsorption, and in our validation Cohort 2, we confirmed enrichment of both proteins and (based on a  $\geq 15\%$  between-group difference and FDRq <1%) identified an action of ACYP1 on renal tubular  $\text{Na}^+\text{-K}^+\text{-ATPase}$  as an additional possible counter-regulatory mechanism.<sup>82</sup> An additional 5 proteins that fulfilled the FDRq <1% and with a  $\geq 10\%$  but <15% between-group difference also have effects on renal tubular ion transport (Supplemental Table 3). Moreover, the action of MYDGF, UMOD, EPO, IGFBP1, OTUB1, HSPA8, and IGBP1 to mitigate podocyte and renal tubular injury (Table 3) may underlie the nephroprotective effects of SGLT2 inhibitors; of note, MYDGF, OTUB1, HSPA8, and IGBP1 were not measured in our discovery Cohort 1. Interestingly, 4 proteins that are differentially enriched by SGLT2 inhibition—thymosin beta-10 (TMSB10), trefoil factor 1 (TFF1), epithelial cell adhesion molecule (EpCAM), and cadherin EGF LAG seven-pass G-type receptor 2 (CELSR2)—promote epithelial cell polarity and thus are poised to play a role in the restoration of renal tubular cell architecture (Supplemental Table 3).<sup>99-102</sup>

Finally, SGLT2 inhibitors have been reported to attenuate sympathetic activation, both experimentally and clinically,<sup>103,104</sup> and the action of differentially-enriched CgA to suppress sympathetic overactivation could contribute to the sympatholytic action and blood pressure-lowering effect of these drugs.<sup>81</sup> The upregulation of KYAT1 (shown in Supplemental Table 3) can also yield sympatholytic effects.<sup>105</sup> Moreover, SGLT2 inhibitors have been reported to improve the function of sarcoplasmic/endoplasmic reticulum  $\text{Ca}^{2+}\text{-ATPase-2a}$  (SERCA2a) to enhance calcium reuptake in the sarcoplasmic reticulum,<sup>106</sup> an action that may be mediated by the effects of MYDGF and ACYP1, whose levels were differentially increased by  $\geq 15\%$  by empagliflozin in our analyses of Cohort 2. In addition, 3 proteins with a FDRq <1% and a between-group difference of  $\geq 10\%$  but <15%—STC1, PPP1R14A, and CDNF—have effects to modulate calcium entry, transport and transients in cardiomyocytes (Supplemental Table 3).<sup>107-109</sup>

**STUDY LIMITATIONS.** The proximity extension assay technology used for our analyses provides normalized protein concentrations that cannot be directly translated to absolute quantification using standard analytic methods. More importantly, it is understood that blood levels of proteins reflect the shedding or secretion of intracellular proteins into the circulation and that the magnitude of extracellular extrusion is not necessarily proportional to a protein's functional

concentration or post-translational activation state in cytosolic subcompartments. Furthermore, the stoichiometry of any concentration-effect relationship is not known, and—accordingly—the  $\geq 10\%$  and  $\geq 15\%$  thresholds we used to identify differentially enriched proteins are arbitrary. Finally, the number of patients who contributed to blood sampling at 52 weeks was far smaller than at 12 weeks and, more importantly, measured between-group differences in physiologically relevant proteins at 52 weeks are typically attenuated because the achievement of a biological target acts (as part of a negative feedback loop) to mute any early surge in the originating stimulus; for example, the initial rise in erythropoietin levels following SGLT2 inhibition subsides toward baseline values simultaneous with a sustained erythrocytosis,<sup>8,110</sup> achieving a new equilibrium set point, even though erythropoietin remains the driving stimulus.

## CONCLUSIONS

In this first validation study of large-scale proteomics in double-blind randomized trial of any treatment in patients with heart failure, our expanded platform was able to confirm the mechanisms identified in our previously reported discovery cohort. The biological signature of the differentially enriched proteins identified in our discovery cohort were replicated and substantially reinforced in our validation cohort. The intriguing replication of the biological signatures across the discovery and validation cohorts is highly consistent with the effects of SGLT2 inhibitors demonstrated in numerous experimental studies. These observations suggest that the effect of SGLT2 inhibitors to promote autophagy and reduce cellular stress; to restore mitochondrial health and ATP production; to promote iron mobilization while enhancing erythropoiesis; to modulate ion reabsorption and maintain the polarity and architecture of the renal tubules; to improve cardiac structure and function; and to attenuate sympathetic overactivity—all demonstrated in experimental studies—are likely relevant to patients with heart failure.

## FUNDING SUPPORT AND AUTHOR DISCLOSURES

The authors met criteria for authorship as described by the International Committee of Medical Journal Editors (ICMJE). No author received payment related to the development of the manuscript. Boehringer Ingelheim was given the opportunity to review the manuscript for medical and scientific accuracy as well as intellectual property considerations. The study was supported and funded by the Boehringer Ingelheim & Eli Lilly and Company Diabetes Alliance. To ensure independent interpretation of clinical trial results and enable authors to fulfill their role and obligations under the ICMJE criteria,

Boehringer Ingelheim grants all external authors access to relevant clinical study data. In adherence with the Boehringer Ingelheim Policy on Transparency and Publication of Clinical Study Data, scientific and medical researchers can request access to clinical study data, typically 1 year after the approval has been granted by major regulatory authorities or after termination of the development program. Researchers should use the <https://vivli.org/> link to request access to study data and visit <https://www.mystudywindow.com/msw/datasharing> for further information. Dr Packer has received consulting fees from 89bio, Abbvie, Actavis, Altimimmune, Ardelyx, ARMGO Pharma, Attralus, Amgen, Alnylam, AstraZeneca, Biopeutics, Boehringer Ingelheim, Caladrius, Casana, Cytokinetics, Eli Lilly & Company, Imara, Moderna, Medtronic, Novartis, Pharmacosmos, Reata, Regeneron, and Salamandra. Dr Ferreira has served as consultant for Boehringer Ingelheim and AstraZeneca. Dr Butler has received consulting fees from Abbott, American Regent, Amgen, Applied Therapeutic, AstraZeneca, Bayer, Boehringer Ingelheim, Bristol Myers Squibb, Cardiac Dimension, Cardior, CVRx, Cytokinetics, Edwards, Element Science, Innolife, Impulse Dynamics, Imbria, Inventiva, Lexicon, Lilly, LivaNova, Janssen, Medtronic, Merck, Occlutech, Novartis, Novo Nordisk, Pfizer, Pharmacosmos, Pharmain, Roche, Sequana, SQ Innovation, and Vifor. Dr Filippatos has received consulting fees from Bayer, Boehringer Ingelheim, and Servier; has received lecture fees from Novartis; has received trial committee membership fees from Impulse Dynamics, Vifor, and Medtronic; has served on trial committee for Cardior; and has received consulting fees from Novo Nordisk. Dr Maldonado has received consulting fees from Boehringer Ingelheim Pharma GmbH & Co KG. Dr Saadati has served as freelance statistician for Boehringer. Dr Sattar has served in advisory positions for Amgen, AstraZeneca, Boehringer Ingelheim, Eli Lilly, Novartis, Novo Nordisk, Pfizer, and Roche Diagnostics; has received consulting fees from Abbott Laboratories, AbbVie, Amgen, AstraZeneca, Boehringer Ingelheim, Eli Lilly, Hanmi Pharmaceuticals, Janssen, Menarini-Ricerche, Novo Nordisk, Pfizer, and Sanofi; has received speaker fees from Abbott Laboratories, AbbVie, AstraZeneca, Boehringer Ingelheim, Eli Lilly, Janssen, Novo Nordisk, and Sanofi; and has received research grants from AstraZeneca, Boehringer Ingelheim, Novartis, and Roche Diagnostics. Dr Anker has received grants and personal fees from Vifor and Abbott Laboratories; has received personal fees for consultancies, trial committee work and lectures from Actimed, AstraZeneca, Bayer, Bioventrix, Boehringer Ingelheim, Brahms, Cardiac Dimensions, Cardior, Cordio, CVRx, Cytokinetics, Edwards, Farraday Pharmaceuticals, GSK, HeartKinetics, Impulse Dynamics, Medtronic, Novartis, Novo Nordisk, Occlutech, Pfizer, Regeneron, Relaxera, Repairon, Scirent, Sensible Medical, Servier, Vectorious, and V-Wave; and is named co-inventor of 2 patent applications regarding MR-proANP (DE 102007010834 & DE 102007022367), but he does not benefit personally from the related issued patents. Drs Gonzalez Maldonado, Panova-Noeva, Prochaska, Saadati, and Sumin are employees of Boehringer Ingelheim. Dr Zannad has served on the Steering Committee or Data Safety Monitoring Board for or served as a consultant to 89bio, Applied Therapeutics, Bayer, Betagenon, Biopeutics, Boehringer Ingelheim, Bristol Myers Squibb, CVRx, Cardior, Cerenon, Cellprothera, CEVA, Merck, Northsea, Novartis, NovoNordisk, Otsuka, Owkin, Salubris, and Servier; has equity in Cardior, G3Pharmaceutical, Cerenon Pharmaceutical, and CVCT; and has lectured for Bayer, Boehringer Ingelheim, CVRx, CEVA, Merck, and Novartis. All other authors have no relationships relevant to the contents of this paper to disclose.

**ADDRESS FOR CORRESPONDENCE:** Dr Milton Packer, Baylor Heart and Vascular Institute, Baylor University Medical Center, 621 North Hall Street, Dallas, Texas 75226, USA. E-mail: [milton.packer@baylorhealth.edu](mailto:milton.packer@baylorhealth.edu).

## REFERENCES

- Vaduganathan M, Docherty KF, Claggett BL, et al. SGLT-2 inhibitors in patients with heart failure: a comprehensive meta-analysis of five randomised controlled trials. *Lancet*. 2022;400:757-767.
- Packer M. Critical reanalysis of the mechanisms underlying the cardiorenal benefits of SGLT2 inhibitors and reaffirmation of the nutrient deprivation signaling/autophagy hypothesis. *Circulation*. 2022;146:1383-1405.
- Packer M. Autophagy-dependent and -independent modulation of oxidative and organellar stress in the diabetic heart by glucose-lowering drugs. *Cardiovasc Diabetol*. 2020;19(1):62. <https://doi.org/10.1186/s12933-020-01041-4>
- Packer M. SGLT2 inhibitors: role in protective reprogramming of cardiac nutrient transport and metabolism. *Nat Rev Cardiol*. 2023;20:443-462.
- Packer M, Wilcox CS, Testani JM. Critical analysis of the effects of SGLT2 inhibitors on renal tubular sodium, water and chloride homeostasis and their role in influencing heart failure outcomes. *Circulation*. 2023;148:354-372.
- Packer M. How can sodium-glucose cotransporter 2 inhibitors stimulate erythrocytosis in patients who are iron-deficient? Implications for understanding iron homeostasis in heart failure. *Eur J Heart Fail*. 2022;24:2287-2296.
- Wee CF, Teo YH, Teo YN, et al. Effects of sodium/glucose cotransporter 2 (SGLT2) inhibitors on cardiac imaging parameters: a systematic review and meta-analysis of randomized controlled trials. *J Cardiovasc Imaging*. 2022;30:153-168.
- Zannad F, Ferreira JP, Butler J, et al. Effect of empagliflozin on circulating proteomics in heart failure: mechanistic insights into the EMPEROR programme. *Eur Heart J*. 2022;43:4991-5002.
- PEA-a high-multiplex immunoassay technology with qPCR or NGS readout. In. 2020. <https://www.olink.com/content/uploads/2021/09/olink-white-paper-pea-a-high-multiplex-immunoassay-technology-with-qpcr-or-ngs-readout-v1.0.pdf>
- Green GH, Diggle PJ. On the operational characteristics of the Benjamini and Hochberg false discovery rate procedure. *Stat Appl Genet Mol Biol*. 2007;6:Article27. <https://doi.org/10.2202/1544-6115.1302>
- Abdellatif M, Trummer-Herbst V, Heberle AM, et al. Fine-tuning cardiac insulin-like growth factor 1 receptor signaling to promote health and longevity. *Circulation*. 2022;145:1853-1866.
- Vasylyeva TL, Ferry RJ Jr. Novel roles of the IGF-IGFBP axis in etiopathophysiology of diabetic nephropathy. *Diabetes Res Clin Pract*. 2007;76:177-186.
- Tang X, Jiang H, Lin P, et al. Insulin-like growth factor binding protein-1 regulates HIF-1 $\alpha$  degradation to inhibit apoptosis in hypoxic cardiomyocytes. *Cell Death Discov*. 2021;7(1):242. <https://doi.org/10.1038/s41420-021-00629-3>
- Hammerling BC, Najor RH, Cortez MQ, et al. A Rab5 endosomal pathway mediates Parkin-dependent mitochondrial clearance. *Nat Commun*. 2017;8:14050. <https://doi.org/10.1038/ncomms14050>
- Huang X, Zhang J, Wang W, Huang Z, Han P. Vps4a regulates autophagic flux to prevent hypertrophic cardiomyopathy. *Int J Mol Sci*. 2023;24(13):10800. <https://doi.org/10.3390/ijms241310800>
- Zaglia T, Milan G, Ruhs A, et al. Atrogin-1 deficiency promotes cardiomyopathy and premature death via impaired autophagy. *J Clin Invest*. 2014;124:2410-2424.
- Wang J, Fang N, Xiong J, Du Y, Cao Y, Ji WK. An ESCRT-dependent step in fatty acid transfer from lipid droplets to mitochondria through VPS13D-TSG101 interactions. *Nat Commun*. 2021;12(1):1252. <https://doi.org/10.1038/s41467-021-21525-5>
- Mackie TD, Kim BY, Subramanya AR, et al. The endosomal trafficking factors CORVET and ESCRT suppress plasma membrane residence of the renal outer medullary potassium channel (ROMK). *J Biol Chem*. 2018;293:3201-3217.
- Zhao L, Wang X, Yu Y, et al. OTUB1 protein suppresses mTOR complex 1 (mTORC1) activity by deubiquitinating the mTORC1 inhibitor DEPTOR. *J Biol Chem*. 2018;293:4883-4892.
- Kuang E, Qi J, Ronai Z. Emerging roles of E3 ubiquitin ligases in autophagy. *Trends Biochem Sci*. 2013;38:453-460.
- Zhong X, Wang T, Zhang W, et al. ERK/RSK-mediated phosphorylation of Y-box binding protein-1 aggravates diabetic cardiomyopathy by suppressing its interaction with deubiquitinase OTUB1. *J Biol Chem*. 2022;298:101989.
- Dong W, Wang H, Shahzad K, et al. Activated protein C ameliorates renal ischemia-reperfusion injury by restricting Y-box binding protein-1 ubiquitination. *J Am Soc Nephrol*. 2015;26:2789-2799.
- Arndt V, Dick N, Tawo R, et al. Chaperone-assisted selective autophagy is essential for muscle maintenance. *Curr Biol*. 2010;20:143-148.
- Le NT, Takei Y, Shishido T, et al. p90RSK targets the ERK5-CHIP ubiquitin E3 ligase activity in diabetic hearts and promotes cardiac apoptosis and dysfunction. *Circ Res*. 2012;110:536-550.
- Zhang C, Xu Z, He XR, Michael LH, Patterson C. CHIP, a cochaperone/ubiquitin ligase that regulates protein quality control, is required for maximal cardioprotection after myocardial infarction in mice. *Am J Physiol Heart Circ Physiol*. 2005;288:H2836-H2842.
- Schisler JC, Rubel CE, Zhang C, Lockyer P, Cyr DM, Patterson C. CHIP protects against cardiac pressure overload through regulation of AMPK. *J Clin Invest*. 2013;123:3588-3599.
- Qi H, Deng F, Wang Y, Zhang H, Kanwar YS, Dai Y. Myo-inositol supplementation alleviates cisplatin-induced acute kidney injury via inhibition of ferroptosis. *Cells*. 2022;12(1):16. <https://doi.org/10.3390/cells12010016>
- Zhang H, Deng Z, Wang Y, et al. CHIP protects against septic acute kidney injury by inhibiting NLRP3-mediated pyroptosis. *iScience*. 2023;26(10):107762. <https://doi.org/10.1016/j.isci.2023.107762>
- Terada K, Ohtsuka K, Imamoto N, Yoneda Y, Mori M. Role of heat shock cognate 70 protein in import of ornithine transcarbamylase precursor into mammalian mitochondria. *Mol Cell Biol*. 1995;15:3708-3713.
- Qiu XB, Shao YM, Miao S, Wang L. The diversity of the DnaJ/Hsp40 family, the crucial partners for Hsp70 chaperones. *Cell Mol Life Sci*. 2006;63:2560-2570.
- Forghani P, Rashid A, Sun F, et al. Carfilzomib treatment causes molecular and functional alterations of human induced pluripotent stem cell-derived cardiomyocytes. *J Am Heart Assoc*. 2021;10(24):e022247. <https://doi.org/10.1161/JAHA.121.022247>
- Mikkelsen H, Vikse BE, Eikrem O, et al. Glomerular proteomic profiling of kidney biopsies with hypertensive nephropathy reveals a signature of disease progression. *Hypertens Res*. 2023;46:144-156.
- Hammond CM, Bao H, Hendriks IA, et al. DNAJC9 integrates heat shock molecular chaperones into the histone chaperone network. *Mol Cell*. 2021;81:2533-2548.
- Balachandra V, Shrestha RL, Hammond CM, et al. DNAJC9 prevents CENP-A mislocalization and chromosomal instability by maintaining the fidelity of histone supply chains. *EMBO J*. 2024;43(11):2166-2197. <https://doi.org/10.1038/s44318-024-00093-6>
- Drake JI, Gomez-Arroyo J, Dumur CI, et al. Chronic carvedilol treatment partially reverses the right ventricular failure transcriptional profile in experimental pulmonary hypertension. *Physiol Genomics*. 2013;45:449-461.
- Zhao Y, Sun M. Metformin rescues Parkin protein expression and mitophagy in high glucose-challenged human renal epithelial cells by inhibiting NF- $\kappa$ B via PP2A activation. *Life Sci*. 2020;246:117382. <https://doi.org/10.1016/j.lfs.2020.117382>
- Yoon S, Kook T, Min HK, et al. PP2A negatively regulates the hypertrophic response by dephosphorylating HDAC2 S394 in the heart. *Exp Mol Med*. 2018;50:1-14.
- Li L, Fang C, Xu D, Xu Y, Fu H, Li J. Cardiomyocyte specific deletion of PP2A causes cardiac hypertrophy. *Am J Transl Res*. 2016;8:1769-1779.
- Grech G, Blázquez-Domingo M, Kolbus A, et al. Igbp1 is part of a positive feedback loop in stem cell factor-dependent, selective mRNA translation initiation inhibiting erythroid differentiation. *Blood*. 2008;112:2750-2760.
- Keceli G, Gupta A, Sourdon J, et al. Mitochondrial creatine kinase attenuates pathologic remodeling in heart failure. *Circ Res*. 2022;130:741-759.
- Whittington HJ, Ostrowski PJ, McAndrew DJ, et al. Over-expression of mitochondrial creatine kinase in the murine heart improves functional

- recovery and protects against injury following ischaemia-reperfusion. *Cardiovasc Res.* 2018;114:858-869.
42. Friedman DL, Perryman MB. Compartmentation of multiple forms of creatine kinase in the distal nephron of the rat kidney. *J Biol Chem.* 1991;266:22404-22410.
43. Kuznetsov AV, Javadov S, Guzun R, Grimm M, Saks V. Cytoskeleton and regulation of mitochondrial function: the role of beta-tubulin II. *Front Physiol.* 2013;4:82. <https://doi.org/10.3389/fphys.2013.00082>
44. Kuznetsov AV, Javadov S, Grimm M, Margreiter R, Ausserlechner MJ, Hagenbuchner J. Crosstalk between mitochondria and cytoskeleton in cardiac cells. *Cells.* 2020;9(1):222. <https://doi.org/10.3390/cells9010222>
45. Bagur R, Tanguy S, Foriel S, et al. The impact of cardiac ischemia/reperfusion on the mitochondria-cytoskeleton interactions. *Biochim Biophys Acta.* 2016;1862:1159-1171.
46. Yancey DM, Guichard JL, Ahmed MI, et al. Cardiomyocyte mitochondrial oxidative stress and cytoskeletal breakdown in the heart with a primary volume overload. *Am J Physiol Heart Circ Physiol.* 2015;308:H651-H663.
47. Wu JW, Hu H, Hua JS, Ma LK. ATPase inhibitory factor 1 protects the heart from acute myocardial ischemia/reperfusion injury through activating AMPK signaling pathway. *Int J Biol Sci.* 2022;18:731-741.
48. Lefebvre V, Du Q, Baird S, et al. Genome-wide RNAi screen identifies ATPase inhibitory factor 1 (ATPIF1) as essential for PARK2 recruitment and mitophagy. *Autophagy.* 2013;9:1770-1779.
49. Shah DI, Takahashi-Makise N, Cooney JD, et al. Mitochondrial Atp1f1 regulates heme synthesis in developing erythroblasts. *Nature.* 2012;491:608-612.
50. Schaap FG, Binas B, Danneberg H, van der Vusse GJ, Glatz JF. Impaired long-chain fatty acid utilization by cardiac myocytes isolated from mice lacking the heart-type fatty acid binding protein gene. *Circ Res.* 1999;85:329-337.
51. Zelencova-Gopejkeno D, Videja M, Grandane A, et al. Heart-type fatty acid binding protein binds long-chain acylcarnitines and protects against lipotoxicity. *Int J Mol Sci.* 2023;24(6):5528. <https://doi.org/10.3390/ijms24065528>
52. Liu ZZ, Hong CG, Hu WB, et al. Autophagy receptor OPTN (optineurin) regulates mesenchymal stem cell fate and bone-fat balance during aging by clearing FABP3. *Autophagy.* 2021;17:2766-2782.
53. Gao S, Li G, Shao Y, et al. FABP5 deficiency impairs mitochondrial function and aggravates pathological cardiac remodeling and dysfunction. *Cardiovasc Toxicol.* 2021;21:619-629.
54. Lin CH, Chang HH, Lai CR, et al. Fatty acid binding protein 6 inhibition decreases cell cycle progression, migration and autophagy in bladder cancers. *Int J Mol Sci.* 2022;23(4):2154. <https://doi.org/10.3390/ijms23042154>
55. Fang CY, Chen MC, Chang TH, et al. Id1 and Hmgcs2 are affected by stretch in HL-1 atrial myocytes. *Int J Mol Sci.* 2018;19(12):4094. <https://doi.org/10.3390/ijms19124094>
56. Calderon RM, Smith CA, Miedzybrodzka EL, et al. Intestinal enteroendocrine cell signaling: retinol-binding protein 2 and retinoid actions. *Endocrinology.* 2022;163:bqac064. <https://doi.org/10.1210/endo/bqac064>
57. Beak JY, Kang HS, Huang W, et al. The nuclear receptor ROR $\alpha$  preserves cardiomyocyte mitochondrial function by regulating caveolin-3-mediated mitophagy. *J Biol Chem.* 2021;297(6):101358. <https://doi.org/10.1016/j.jbc.2021.101358>
58. Da Silva F, Jian Motamedi F, Weerasinghe Arachchige LC, et al. Retinoic acid signaling is directly activated in cardiomyocytes and protects mouse hearts from apoptosis after myocardial infarction. *Elife.* 2021;10:e68280. <https://doi.org/10.7554/eLife.68280>
59. Wu J, Zheng C, Wan X, et al. Retinoic acid alleviates cisplatin-induced acute kidney injury through activation of autophagy. *Front Pharmacol.* 2020;11:987. <https://doi.org/10.3389/fphar.2020.00987>
60. Xu W, Barrientos T, Mao L, Rockman HA, Saue AA, Andrews NC. Lethal cardiomyopathy in mice lacking transferrin receptor in the heart. *Cell Rep.* 2015;13:533-545.
61. Crane FL, Navas P, Low H, Sun IL, de Cabo R. Sirtuin activation: a role for plasma membrane in the cell growth puzzle. *J Gerontol A Biol Sci Med Sci.* 2013;68:368-370.
62. Lin C, Zhang M, Zhang Y, et al. Helix B surface peptide attenuates diabetic cardiomyopathy via AMPK-dependent autophagy. *Biochem Biophys Res Commun.* 2017;482:665-671.
63. Cui L, Guo J, Zhang Q, et al. Erythropoietin activates SIRT1 to protect human cardiomyocytes against doxorubicin-induced mitochondrial dysfunction and toxicity. *Toxicol Lett.* 2017;275:28-38.
64. Li K, Gao L, Zhou S, et al. Erythropoietin promotes energy metabolism to improve LPS-induced injury in HK-2 cells via SIRT1/PGC1- $\alpha$  pathway. *Mol Cell Biochem.* 2023;478:651-663.
65. Hu MC, Shi M, Cho HJ, et al. The erythropoietin receptor is a downstream effector of Klotho-induced cytoprotection. *Kidney Int.* 2013;84:468-481.
66. Su YY, Gordon CT, Ye TZ, Perkins AC, Chui DH. Human ERMAP: an erythroid adhesion/receptor transmembrane protein. *Blood Cells Mol Dis.* 2001;27:938-949.
67. Blekkenhorst GH, Eales L, Pimstone NR. Activation of uroporphyrinogen decarboxylase by ferrous iron in porphyria cutanea tarda. *S Afr Med J.* 1979;4(56):918-920.
68. Mukerji SK, Pimstone NR. Free radical mechanism of oxidation of uroporphyrinogen in the presence of ferrous iron. *Arch Biochem Biophys.* 1990;281:177-184.
69. Fernández-Tomé MC, Billi de Catabbi SC, Aldonatti C, San Martin de Viale LC, Sterin-Speziale NB. Heme metabolism and lipid peroxidation in rat kidney hexachlorobenzene-induced porphyria: a compartmentalized study of biochemical pathogenic mechanisms. *Kidney Blood Press Res.* 2000;23:20-26.
70. Mahoney-Sanchez L, Bouchaoui H, Boussaad I, et al. Alpha synuclein determines ferroptosis sensitivity in dopaminergic neurons via modulation of ether-phospholipid membrane composition. *Cell Rep.* 2022;40(8):111231. <https://doi.org/10.1016/j.celrep.2022.111231>
71. Zhao ST, Qiu ZC, Zeng RY, et al. Exploring the molecular biology of ischemic cardiomyopathy based on ferroptosis-related genes. *Exp Ther Med.* 2024;27(5):221. <https://doi.org/10.3892/etm.2024.12509>
72. Bozic M, Caus M, Rodrigues-Diez RR, et al. Protective role of renal proximal tubular alpha-synuclein in the pathogenesis of kidney fibrosis. *Nat Commun.* 2020;11(1):1943. <https://doi.org/10.1038/s41467-020-15732-9>
73. Korf-Klingebiel M, Reboll MR, Polten F, et al. Myeloid-derived growth factor protects against pressure overload-induced heart failure by preserving sarco/endoplasmic reticulum Ca(2+)-ATPase expression in cardiomyocytes. *Circulation.* 2021;144:1227-1240.
74. Korf-Klingebiel M, Reboll MR, Klede S, et al. Myeloid-derived growth factor (C19orf10) mediates cardiac repair following myocardial infarction. *Nat Med.* 2015;21:140-149.
75. Wang Y, Li Y, Feng J, et al. Myd88 promotes cardiomyocyte proliferation and neonatal heart regeneration. *Theranostics.* 2020;10:9100-9112.
76. Du P, Wang T, Wang H, Yang M, Yin H. Mucin-fused myeloid-derived growth factor (MYDGF164) exhibits a prolonged serum half-life and alleviates fibrosis in chronic kidney disease. *Br J Pharmacol.* 2022;179:4136-4156.
77. Zhan P, Zhang Y, Shi W, et al. Myeloid-derived growth factor deficiency exacerbates mitotic catastrophe of podocytes in glomerular disease. *Kidney Int.* 2022;102:546-559.
78. Tota B, Cerra MC, Gattuso A. Catecholamines, cardiac natriuretic peptides and chromogranin A: evolution and physiopathology of a 'whip-brake' system of the endocrine heart. *J Exp Biol.* 2010;213:3081-3103.
79. Alam MJ, Gupta R, Mahapatra NR, Goswami SK. Catestatin reverses the hypertrophic effects of norepinephrine in H9c2 cardiac myoblasts by modulating the adrenergic signaling. *Mol Cell Biochem.* 2020;464:205-219.
80. Lener D, Noflatscher M, Kirchmair E, et al. The angiogenic neuropeptide catestatin exerts beneficial effects on human coronary vascular cells and cardiomyocytes. *Peptides.* 2023;168:171077. <https://doi.org/10.1016/j.peptides.2023.171077>
81. Rao F, Wen G, Gayen JR, et al. Catecholamine release-inhibitory peptide catestatin (chromogranin A[352-372]): naturally occurring amino acid variant Gly364Ser causes profound changes in human autonomic activity and alters risk for hypertension. *Circulation.* 2007;115:2271-2281.
82. Tadini-Buoninsegni F, Nassi P, Nediani C, Dolfi A, Guidelli R. Investigation of Na(+),K(+)-ATPase on a solid supported membrane: the role of acylphosphatase on the ion transport mechanism. *Biochim Biophys Acta.* 2003;1611:70-80.

83. Nediani C, Fiorillo C, Rigacci S, et al. A novel interaction mechanism accounting for different acylphosphatase effects on cardiac and fast twitch skeletal muscle sarcoplasmic reticulum calcium pumps. *FEBS Lett.* 1999;443(3):308-312.
84. Cai H, Wu L, Qu W, et al. Regulation of apical NHE3 trafficking by ouabain-induced activation of basolateral Na/K-ATPase receptor complex. *Am J Physiol Cell Physiol.* 2008;294:C555-C563.
85. Nediani C, Formigli L, Perna AM, et al. Early changes induced in the left ventricle by pressure overload: an experimental study on swine heart. *J Mol Cell Cardiol.* 2000;32:131-142.
86. Mutig K, Kahl T, Saritas T, et al. Activation of the bumetanide-sensitive Na<sup>+</sup>, K<sup>+</sup>, 2Cl<sup>-</sup> cotransporter (NKCC2) is facilitated by Tamm-Horsfall protein in a chloride-sensitive manner. *J Biol Chem.* 2011;286:30200-30210.
87. Kemter E, Fröhlich T, Arnold GJ, Wolf E, Wanke R. Mitochondrial dysregulation secondary to endoplasmic reticulum stress in autosomal dominant tubulointerstitial kidney disease-UMOD (ADTKD-UMOD). *Sci Rep.* 2017;7:42970. <https://doi.org/10.1038/srep42970>
88. Liu Y, El-Achkar TM, Wu XR. Tamm-Horsfall protein regulates circulating and renal cytokines by affecting glomerular filtration rate and acting as a urinary cytokine trap. *J Biol Chem.* 2012;287:16365-16378.
89. Krishnan D, Liu L, Wiebe SA, Casey JR, Cordat E, Alexander RT. Carbonic anhydrase II binds to and increases the activity of the epithelial sodium-proton exchanger, NHE3. *Am J Physiol Renal Physiol.* 2015;309:F383-F392.
90. Montecucco F, Braunersreuther V, Lenglet S, et al. CC chemokine CCL5 plays a central role impacting infarct size and post-infarction heart failure in mice. *Eur Heart J.* 2012;33:1964-1974.
91. Hossain S, Gilani A, Pascale J, et al. Gpr75-deficient mice are protected from high-fat diet-induced obesity. *Obesity (Silver Spring).* 2023;31:1024-1037.
92. Chen Z, Haus JM, Chen L, et al. CCL28-induced CCR10/eNOS interaction in angiogenesis and skin wound healing. *FASEB J.* 2020;34:5838-5850.
93. Cencer CS, Robinson KL, Tyska MJ. Loss of intermicrovillar adhesion impairs basolateral junctional complexes in transporting epithelia. *This article was posted as a preprint on bioRxiv on.* March 19, 2024. <https://doi.org/10.1101/2024.03.19.585733>
94. Abdellatif M, Montégut L, Kroemer G. Actionable autophagy checkpoints in cardiovascular ageing. *Eur Heart J.* 2023;44:4819-4821.
95. Josephrajan A, Hertz AV, Bohm EK, et al. Unconventional secretion of adipocyte fatty acid binding protein 4 is mediated by autophagic proteins in a sirtuin-1-dependent manner. *Diabetes.* 2019;68:1767-1777.
96. Zheng T, Waqng -Y, Chen Y, et al. Src activation aggravates podocyte injury in diabetic nephropathy via suppression of FUNDC1-mediated mitophagy. *Front Pharmacol.* 2022;13:897046. <https://doi.org/10.3389/fphar.2022.897046>
97. Anandhan A, Chen W, Nguyen N, Madhavan L, Dodson M, Zhang DD. alpha-Syn overexpression, NRF2 suppression, and enhanced ferroptosis create a vicious cycle of neuronal loss in Parkinson's disease. *Free Radic Biol Med.* 2022;192:130-140.
98. Ünal İ, Cansız D, Beler M, Sezer Z, Güzel E, Emekli-Alturfan E. Sodium-dependent glucose co-transporter-2 inhibitor empagliflozin exerts neuroprotective effects in rotenone-induced Parkinson's disease model in zebrafish; mechanism involving ketogenesis and autophagy. *Brain Res.* 2023;1820:148536. <https://doi.org/10.1016/j.brainres.2023.148536>
99. Gerosa C, Fanni D, Nemolato S, et al. Thymosin beta-10 expression in developing human kidney. *J Matern Fetal Neonatal Med.* 2010;23(Suppl 3):125-128.
100. Nieskens TTT, Persson M, Kelly EJ, Sjögren AK. A multicompartment human kidney proximal tubule-on-a-chip replicates cell polarization-dependent cisplatin toxicity. *Drug Metab Dispos.* 2020;48:1303-1311.
101. Trzpis M, McLaughlin PM, van Goor H, et al. Expression of EpCAM is up-regulated during regeneration of renal epithelia. *J Pathol.* 2008;216:201-208.
102. Shima Y, Copeland NG, Gilbert DJ, et al. Differential expression of the seven-pass transmembrane cadherin genes *Celsr1-3* and distribution of the *Celsr2* protein during mouse development. *Dev Dyn.* 2002;223:321-332.
103. Zhang N, Feng B, Ma X, Sun K, Xu G, Zhou Y. Dapagliflozin improves left ventricular remodeling and aorta sympathetic tone in a pig model of heart failure with preserved ejection fraction. *Cardiovasc Diabetol.* 2019;18(1):107. <https://doi.org/10.1186/s12933-019-0914-1>
104. Scholtes RA, Mosterd CM, Hesp AC, Smits MM, Heerspink HJL, van Raalte DH. Mechanisms underlying the blood pressure-lowering effects of empagliflozin, losartan and their combination in people with type 2 diabetes: a secondary analysis of a randomized crossover trial. *Diabetes Obes Metab.* 2023;25:198-207.
105. Vayssettes-Courchay C, Bouysset F, Verbeuren TJ, Laubie M. Evidence against the involvement of the nucleus tractus solitarius in the sympatholytic effect of 8-hydroxy-2-(di-n-propylamino)tetralin in the cat. *Eur J Pharmacol.* 1995;285:299-304.
106. Hammoudi N, Jeong D, Singh R, et al. Empagliflozin improves left ventricular diastolic dysfunction in a genetic model of type 2 diabetes. *Cardiovasc Drugs Ther.* 2017;31:233-246.
107. Sheikh-Hamad D, Bick R, et al. Stanniocalcin-1 is a naturally occurring L-channel inhibitor in cardiomyocytes: relevance to human heart failure. *Am J Physiol Heart Circ Physiol.* 2003;285:H442-H448.
108. Li Z, Yu L, Zhang Y, et al. Identification of human, mouse and rat PPP1R14A, protein phosphatase-1 inhibitor subunit 14A, & mapping human PPP1R14A to chromosome 19q13.13-q13.2. *Mol Biol Rep.* 2001;28:91-101.
109. Liu H, Yu C, Yu H, et al. Cerebral dopamine neurotrophic factor protects H9c2 cardiomyocytes from apoptosis. *Herz.* 2018;43:346-351.
110. Mazer CD, Hare GMT, Connelly PW, et al. Effect of empagliflozin on erythropoietin levels, iron stores, and red blood cell morphology in patients with type 2 diabetes mellitus and coronary artery disease. *Circulation.* 2020;141:704-707.

---

**KEY WORDS** autophagy, empagliflozin, heart failure, iron, mitochondria, proteomics, SGLT2 inhibitors

---

**APPENDIX** For supplemental methods and tables, please see the online version of this paper.